FIG. 4. TBS-induced LTP in area CA1 of the *gad* mouse hippocampus was impaired. (A) LTP induced by TBS in wild-type (O) and *gad* (O) mice. The fEPSP slope was normalized to baseline (pre-TBS) values. Typical fEPSP traces are shown above. Traces were recorded (a) just before TBS, (b) immediately after TBS and (c) 45 min after TBS. (B) Tetanus-induced LTP was identical in wild-type and *gad* mice.
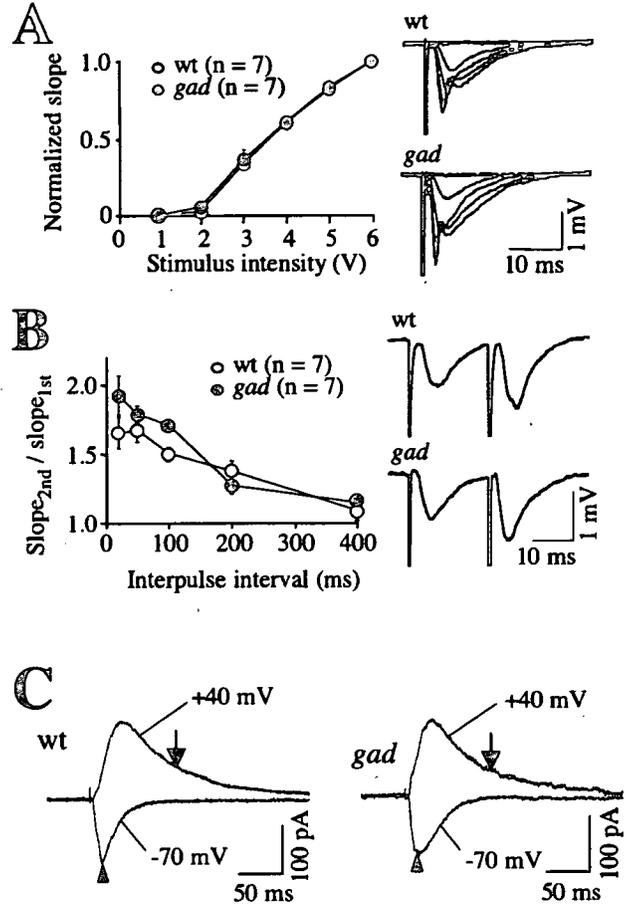
FIG. 5. Stimulus–output curves, paired-pulse facilitation and NMDA receptor–mediated currents were similar in wild-type and *gad* mice. (A) The relation between stimulus intensity and the slope of the fEPSP was identical in wild-type and *gad* mice. For each slice, fEPSP slopes elicited by six different stimulus intensities (1–6 V; sample traces in the right panel) were normalized to the value obtained using 6-V stimulation, and then normalized values were averaged. (B) Paired-pulse facilitation of fEPSPs did not differ substantially between wild-type and *gad* mice. (C) The ratio of NMDA receptor-mediated currents to non-NMDA receptor-mediated currents was identical in wild-type and *gad* mice. Patch-clamp recordings from neurons voltage-clamped to −70 and +40 mV. The arrowhead indicates the peak of the non-NMDA receptor-mediated current, and the arrow indicates 100 ms poststimulation for the NMDA receptor-mediated current; current amplitudes at these points were used for the ratio.

post-TBS was 1.43 ± 0.07 (*n* = 5) in the presence of actinomycin D, and this value differed significantly from that in wild-type hippocampal slices without actinomycin D (1.87 ± 0.08, *P* = 0.003; two-tailed Student's *t*-test). This result agrees with a previous report (Nguyen & Kandel, 1997). In contrast, TBS-induced LTP in *gad* mice was insensitive to actinomycin D (Fig. 6B). The normalized fEPSP slope at 45 min post-TBS was 1.36 ± 0.04 (*n* = 5) in the presence of actinomycin D and did not differ significantly from the value in *gad* hippocampal slices without actinomycin D (1.36 ± 0.07, *P* = 0.948; two-tailed Student's *t*-test). These results suggest that a transcription-dependent component of LTP is impaired in *gad* mice. In both

wild-type and *gad* mice, actinomycin D did not affect the baseline fEPSP slope (without TBS) up to 80 min postapplication (Fig. 6C and D).

CREB phosphorylation was altered in gad mice

Late-phase LTP in the hippocampal CA1 field requires transcription elicited by phosphorylation of serine 133 on cAMP response element binding protein (CREB; Nguyen *et al.*, 1994). In addition, Aplysia UCH is involved in persistent activation of PKA during long-term synaptic facilitation (Hedge *et al.*, 1997). From these reports and our experiments using actinomycin D above, we suspected that phosphorylated CREB (pCREB)-induced transcription is disrupted in *gad* mice. To address this, we analysed pCREB in the CA1 field of slices used
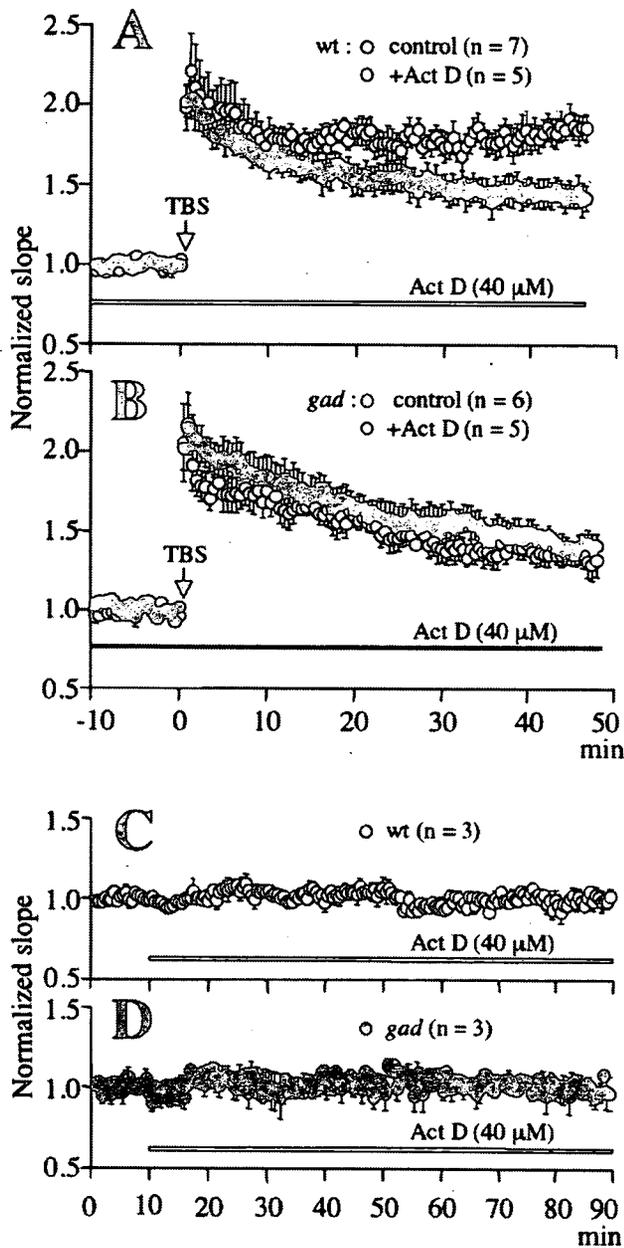
FIG. 6. Transcription-dependent LTP was impaired in *gad* mice. (A and B) Actinomycin D (Act D) suppressed late-phase LTP in (A) wild-type mice but (B) had no effect in *gad* mice. Act D was applied 10 min before LTP induction and was continuously applied until 50 min post-TBS. LTP in the absence of Act D (control) has been reproduced from Fig. 4. (C and D) Without TBS, Act D had no effect on the normalized fEPSP slope in either (C) wild-type or (D) *gad* mice.
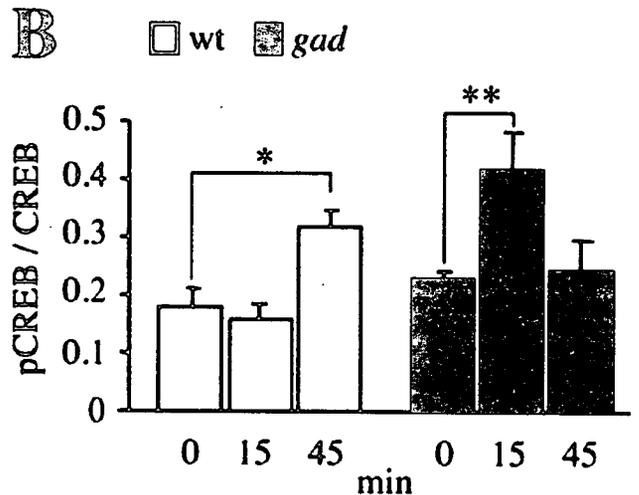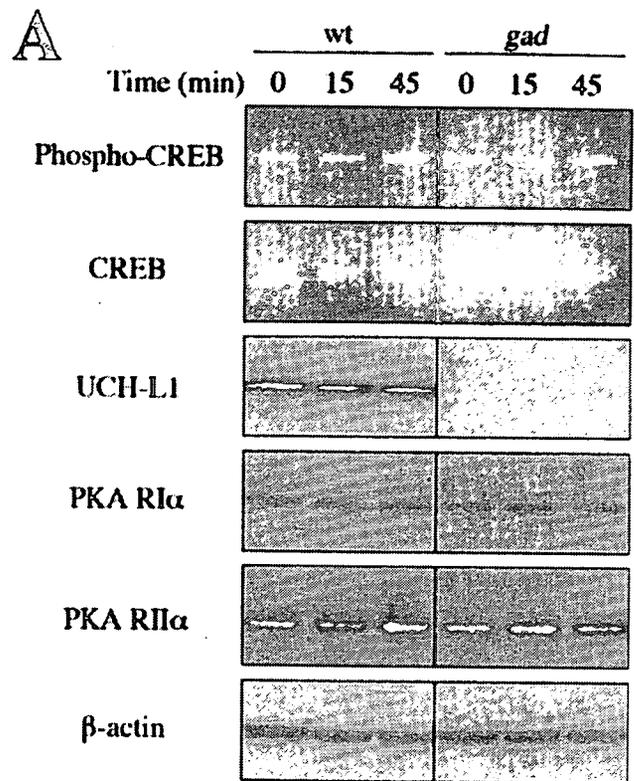
FIG. 7. CREB phosphorylation was altered in *gad* mice. (A) Western blotting of samples prepared from hippocampal slices recovered pre-TBS (0), 15 min post-TBS (15) or 45 min post-TBS (45). Primary antibodies are indicated to the left of the blots. Similar results were obtained at each time point in six slices from wild-type mice and five slices from *gad* mice. (B) The normalized band density of pCREB to CREB at time 0 (pre-TBS), 15 min and 45 min post-TBS in wild-type ($n = 5$) and *gad* ($n = 4$) mice. *$P = 0.012$ and **$P = 0.014$, Bonferroni–Dunn test.

for electrophysiological recording by Western blotting (Fig. 7A). In wild-type mice, pCREB levels at 15 min post-TBS did not differ from pre-TBS levels, but at 45 min post-TBS levels were increased relative to pre-TBS levels. The onset of CREB phosphorylation (45 min postconditioning) is in agreement with a previous report (Ahmed & Frey, 2005). In *gad* mice, however, pCREB levels were increased at 15 min post-TBS but not maintained at 45 min post-TBS (Fig. 7A). Unphosphorylated CREB levels were similar among samples

(Fig. 7A). Similar results were obtained in slices from five wild-type and four *gad* mice. In each set of slices, the band density of pCREB was normalized to that of CREB and the values were averaged (Fig. 7B). In wild-type mice (Fig. 7B), the normalized pCREB levels at 15 min post-TBS did not differ significantly from pre-TBS levels

($P = 0.656$; Bonferroni–Dunn test) but at 45 min post-TBS pCREB levels were significantly higher than pre-TBS levels ($P = 0.012$). In *gad* mice (Fig. 7B), pCREB levels were significantly higher at 15 min post-TBS ($P = 0.014$), but at 45 min post-TBS pCREB levels were not significantly different from pre-TBS levels ($P = 0.393$). These results suggest that the onset and persistence of CREB phosphorylation are altered in *gad* mice.

In Aplysia, serotonin stimulation that induces synaptic plasticity increases expression of UCH by about five-fold. The increased UCH expression stimulates proteasomal degradation of the PKA regulatory subunit N4, thereby inducing persistent PKA activity (Hedge *et al.*, 1997). To determine whether this process also exists in mice, we analysed UCH-L1 and PKA regulatory subunits Iα and IIα in the CA1 field of hippocampal slices by Western blotting. As Fig. 7A shows, the level of UCH-L1 was not obviously affected by TBS at either 15 or 45 min post-TBS in wild-type mice. For quantitative analysis, the band density of UCH-L1 was normalized to that of β-actin and the normalized value was then further normalized to pre-TBS values. At 15 and 45 min post-TBS, the normalized values were 1.00 ± 0.24 ($n = 5$) and 1.06 ± 0.21 ($n = 5$), respectively, confirming that UCH-L1 levels were unchanged. Similarly, TBS-induced changes in the levels of PKA regulatory subunit Iα and IIα were also not apparent in either type of mouse (Fig. 7A). For example, the relative band-density of PKA IIα normalized to β-actin was 1.03 ± 0.14 (15 min post-TBS) and 1.06 ± 0.12 (45 min post-TBS) for wild-type mice ($n = 5$). In *gad* mice ($n = 4$), values were 1.02 ± 0.20 (15 min post-TBS) and 1.01 ± 0.25 (45 min post-TBS). For pre-TBS, the relative band-density of PKA IIα normalized to β-actin also did not differ between wild-type and *gad* mice [the normalized value for *gad* mice/the normalized value for wild-type mice was 0.96 ± 0.10 ($n = 4$)].

Discussion

In this study, we demonstrated that UCH-L1 is required for (i) maintenance of memory in a passive avoidance test and exploratory behaviour in a novel environment, and (ii) a transcription-dependent component of TBS-induced LTP in area CA1 of the hippocampus. UCH-L1 may be essential in transcription-dependent TBS-LTP because it maintains the integrity of TBS-induced CREB phosphorylation. No outstanding forebrain atrophy or aberrant structures were evident in 6-week-old *gad* mice at the level of the light microscope. Thus, the functional abnormalities caused by the lack of UCH-L1 occurred in the absence of any detectable gross structural abnormalities in the brain. However, abnormalities in neuron morphology, such as spine morphology or density, remain a possibility in *gad* mice.

Several studies suggest that synaptic and memory abnormalities precede neuronal cell death in AD (Yao *et al.*, 2003) and in AD model mice (Chapman *et al.*, 1999; Freir *et al.*, 2001; Snyder *et al.*, 2005; Shemer *et al.*, 2006), which supports the hypothesis that synapses may be an initial target in AD (Small *et al.*, 2001; Selkoe, 2002). Aβ is thought to be one of the major players that disrupt synaptic function (reviewed in Selkoe, 2002). Because we have shown here that UCH-L1 is essential for memory maintenance, exploratory behaviour and a particular form of hippocampal LTP, it is possible that the AD-associated reduction in UCH-L1 (Choi *et al.*, 2004) further exacerbates the synaptic and memory deficits induced by Aβ accumulation. In addition, glutamate-induced CREB phosphorylation is decreased by Aβ treatment of cultured hippocampal neurons (Vitolo *et al.*, 2002). Thus, accumulation of Aβ and reduction of UCH-L1 may act cooperatively to disrupt CREB phosphorylation. The recent finding

that introduction of exogenous UCH-L1 into AD model mice rescues synaptic and memory deficits supports this possibility (Gong *et al.*, 2006).

It should be noted that memory deficits are already evident in young *gad* mice (6 weeks of age). Analysis of AD model mice has shown that the onset of the behavioural phenotype is generally much slower. For example, deficits in visible platform recognition become evident by 9 months of age, and deficits in sensorimotor tasks are clearly manifest by 14 months in the Tg2579 transgenic AD model mice (King & Arendash, 2002). Impairments in passive avoidance and small-pool performance are marked only at 18 and 25 months of age in the APP23 transgenic AD model mice (Kelly *et al.*, 2003). It has not been reported whether UCH-L1 is down-regulated in these model mice. In the APP/PS1 mouse model of AD, on the other hand, relatively young (3- to 4-month-old) mice have impaired contextual learning (Trinchese *et al.*, 2004; Gong *et al.*, 2006), and reduced hippocampal UCH activity is evident at 4–6 months of age (Gong *et al.*, 2006). Whether the onset of the reduction in the hydrolase activity is synchronous with the onset of impaired contextual learning in the APP/PS1 mouse is unknown. This information is necessary to further verify the involvement of UCH-L1 in memory deficits associated with AD and in AD model mice.

Impairment of memory in *gad* mice was associated with impaired transcription-dependent LTP in the hippocampus. Because LTP is a well-known cellular mechanism of memory (reviewed in Bliss & Collingridge, 1993), it is reasonable to speculate that impaired LTP is one of the mechanisms underlying the memory deficits in *gad* mice. Our results provide a possible mechanistic link between the lack of UCH-L1 and impaired LTP: alteration of CREB phosphorylation. Proper timing and persistence of CREB phosphorylation are essential for the gene expression required to maintain LTP in area CA1 of the hippocampus (Impey *et al.*, 1996). After conditioning in the passive avoidance test, cAMP response element-mediated transcription is induced in hippocampal area CA1 (Impey *et al.*, 1998). Thus, the alteration of CREB phosphorylation and subsequent failure to maintain LTP might be responsible for reduced performance of *gad* mice in the passive avoidance test. However, LTP at hippocampal CA1 synapses is dependent on NMDA receptors (Harris *et al.*, 1984; Larson & Lynch, 1988). Phosphorylation of CREB is also NMDA receptor-dependent (Ahmed & Frey, 2005). This type of LTP occurs in various brain regions (reviewed in Martin *et al.*, 2000), and UCH-L1 is expressed in almost all brain regions. Therefore, impaired LTP in other brain regions may also be involved in the poor performance of *gad* mice in the passive avoidance test and other behavioural tests. Postsynaptically, the ubiquitin–proteasome system is involved in activity-dependent changes in postsynaptic protein composition and signalling (Ehlers, 2003; reviewed in Yi & Ehlers, 2007). UCH-L1 has *in vitro* enzymatic activity that exposes the free C-terminus of ubiquitin, which is required for protein ubiquitination (Larsen *et al.*, 1998), and monoubiquitin levels are decreased in *gad* mouse brain (Osaka *et al.*, 2003).

In conclusion, we report that UCH-L1 is required for the maintenance of memory in passive avoidance learning, exploratory behaviour and hippocampal CA1 LTP in mice. We propose that UCH-L1-mediated maintenance of the temporal integrity and persistence of CREB phosphorylation is required for CA1 LTP.

Acknowledgements

Abbreviations

Aβ, amyloid β-protein; ACSF, artificial cerebrospinal fluid; AD, Alzheimer's disease; CREB, cyclic AMP response element-binding protein; fEPSPs, field excitatory postsynaptic potentials; *gad*, gracile axonal dystrophy; H&E, hematoxylin and eosin; LTP, long-term potentiation; pCREB, phosphorylated CREB; PD, Parkinson's disease; PKA, protein kinase A; TBS, theta-burst stimulation; UCH-L1, ubiquitin C-terminal hydrolase L1.

References

Abel, T., Nguyen, P.V., Barad, M., Deuel, T.A. & Kandel, E.R. (1997) Genetic demonstration of a role for PKA in the late phase of LTP and in the hippocampus-based long-term memory. *Cell*, **88**, 615–626.

Ahmed, T. & Frey, J.U. (2005) Plasticity-specific phosphorylation of CaMKII, MAP-kinases and CREB during late-LTP in rat hippocampal slices in vitro. *Neuropharmacology*, **49**, 477–492.

Bevilaqua, L., Ardenghi, P., Schroder, N., Bromberg, E., Schmitz, P.K., Schaeffer, E., Quevedo, J., Bianchin, M., Walz, R., Medina, J.H. & Izquierdo, I. (1997) Drugs acting upon the cyclic adenosine monophosphate/protein kinase A signaling pathway modulate memory consolidation when given late after training into rat hippocampus but not amygdala. *Behav. Pharmacol.*, **8**, 331–338.

Bliss, T.V. & Collingridge, G.L. (1993) A synaptic model of memory: long-term potentiation in the hippocampus. *Nature*, **361**, 31–39.

Bouton, M.E., Kenney, F.A. & Rosengard, C. (1990) State-dependent fear extinction with two benzodiazepine tranquilizers. *Behav. Neurosci.*, **104**, 44–55.

Bradshaw, K.D., Emptage, N.L. & Bliss, T.V. (2003) A role for dendritic protein synthesis in hippocampal late LTP. *Eur. J. Neurosci.*, **18**, 3150–3152.

Castegna, A., Aksenov, M., Aksenova, M., Thongboonkerd, V., Klein, J.B., Pierce, W.M., Booze, R., Markesbery, W.M. & Butterfield, D.A. (2002) Proteomic identification of oxidatively modified proteins in Alzheimer's disease brain. Part I: creatine kinase BB, glutamine synthase, and ubiquitin carboxy-terminal hydrolase L-1. *Free Radic. Biol. Med.*, **33**, 562–571.

Chapman, P.F., White, G.L., Jones, M.W., Cooper-Blacketer, D., Marshall, V.J., Irizarry, M., Younkin, L., Good, M.A., Bliss, T.V., Hyman, B.T., Younkin, S.G. & Hsiao, K.K. (1999) Impaired synaptic plasticity and learning in aged amyloid precursor protein transgenic mice. *Nat. Neurosci.*, **2**, 271–276.

Choi, J., Levey, A.I., Weintraub, S.T., Rees, H.D., Gearing, M., Chin, L.S. & Li, L. (2004) Oxidative modifications and down-regulation of ubiquitin carbocyl-terminal hydrolase L1 associated with idiopathic Parkinson's and Alzheimer's diseases. *J. Biol. Chem.*, **279**, 13256–13264.

Ehlers, M.D. (2003) Activity level controls postsynaptic composition and signaling via the ubiquitin-proteasome system. *Nat. Neurosci.*, **6**, 231–242.

Freir, D.B., Holscher, C. & Herron, C.E. (2001) Blockade of long-term potentiation by β-amyloid peptides in the CA1 region of the rat hippocampus in vivo. *J. Neurophysiol.*, **85**, 708–713.

Gong, B., Cao, Z., Zheng, P., Vitolo, O.V., Liu, S., Staniszewski, A., Moolman, D., Zhang, H., Shelanski, M. & Arancio, O. (2006) Ubiquitin hydrolase Uch-L1 rescues beta-amyloid-induced decreases in synaptic function and contextual memory. *Cell*, **126**, 775–788.

Harris, E.W., Ganong, A.H. & Cotman, C.W. (1984) Long-term potentiation in the hippocampus involves activation of N-methyl-D-aspartate receptors. *Brain Res.*, **323**, 132–137.

Hedge, A.N., Inokuchi, K., Pei, W., Casadio, A., Ghirardi, M., Chain, D.G., Martin, K.C., Kandel, E.R. & Schwartz, J.H. (1997) Ubiquitin C-terminal hydrolase is an immediate-early gene essential for long-term facilitation in Aplysia. *Cell*, **89**, 115–126.

Ichihara, N., Wu, J., Chui, D.H., Yamazaki, K., Wakabayashi, T. & Kikuchi, T. (1995) Axonal degeneration promotes abnormal accumulation of amyloid beta-protein in ascending gracile tract of gracile axonal dystrophy (*GAD*) mouse. *Brain Res.*, **695**, 173–178.

Impey, S., Mark, M., Villacres, E.C., Poser, S., Chavkin, C. & Storm, D.R. (1996) Induction of CRE-mediated gene expression by stimuli that generate long-lasting LTP in area CA1 of the hippocampus. *Neuron*, **16**, 973–982.

Impey, S., Smith, D.M., Obrietan, K., Donahue, R., Wade, C. & Storm, D.R. (1998) Stimulation of cAMP response element (CRE)-mediated transcription during contextual learning. *Nat. Neurosci.*, **1**, 595–601.

Kabuta, T., Suzuki, Y. & Wada, K. (2006) Degradation of amyotrophic lateral sclerosis-linked mutant Cu, Zn-superoxide dismutase proteins by macro-autophagy and the proteasome. *J. Biol. Chem.*, **281**, 30524–30533.

Kelly, P.H., Bondolfi, L., Hunziker, D., Schlecht, H.-P., Carver, K., Maguire, E., Arbamowski, D., Wiederhold, K.-H., Sturchler-Pierrat, C., Jucker, M., Bergmann, R., Staufenbiel, M. & Sommer, B. (2003) Progressive age-related impairment of cognitive behavior in APP23 transgenic mice. *Neurobiol. Aging*, **24**, 365–378.

Kikuchi, T., Mukoyama, M., Yamazaki, K. & Moriya, H. (1990) Axonal degeneration of ascending sensory neurons in gracile axonal dystrophy mutant mouse. *Acta Neuropathol.*, **80**, 145–151.

King, D.L. & Arendash, G.W. (2002) Behavioral characterization of the Tg2576 transgenic model of Alzheimer's disease through 19 months. *Physiol. Behav.*, **75**, 627–642.

Larsen, C.N., Krantz, B.A. & Wilkinson, K.D. (1998) Substrate specificity of deubiquitinating enzyme: ubiquitin C-terminal hydrolases. *Biochemistry*, **37**, 3358–3368.

Larson, J. & Lynch, G. (1988) Role of N-methyl-D-aspartate receptors in the induction of synaptic potentiation by burst stimulation patterned after the hippocampal theta-rhythm. *Brain Res.*, **441**, 111–118.

Leroy, E., Boyer, R., Auburger, G., Leube, B., Ulm, G., Mezey, E., Harta, G., Brownstein, M.J., Jonnalagada, S., Chernova, T., Dehejia, A., Lavedan, C., Gasser, T., Steinbach, P.J., Wilkinson, K.D. & Polymeropoulos, M.H. (1998) The ubiquitin pathway in Parkinson's disease. *Nature*, **395**, 451–452.

Lever, C., Burton, S. & O'Keefe, L. (2006) Rearing on hind legs, environmental novelty, and the hippocampal formation. *Rev. Neurosci.*, **17**, 111–133.

Liu, Y.C., Fallon, L., Lashuei, H.A., Liu, Z.H. & Lansbury,P.T. Jr (2002) The UCH-L1 gene encodes two opposing enzymatic activities that affect alpha-synuclein degradation and Parkinson's disease susceptibility. *Cell*, **111**, 209–218.

Malinow, R. & Malenka, R.C. (2002) AMPA receptor trafficking and synaptic plasticity. *Annu. Rev. Neurosci.*, **25**, 103–126.

Maraganore, D.M., Farrer, M.J., Hardly, J.A., Lincoln, S.J., McDonnell, S.K. & Rocca, W.A. (1999) Case-control study of the ubiquitin carboxy-terminal hydrolase L1 gene in Parkinson's disease. *Neurology*, **53**, 1858–1860.

Martin, S.J., Grimwood, P.D. & Morris, R.G.M. (2000) Synaptic plasticity and memory. *Annu. Rev. Neurosci.*, **23**, 649–711.

Morris, R.G., Garrud, P., Rawlins, J.N. & O'Keefe, J. (1982) Place navigation impaired in rats with hippocampal lesions. *Nature*, **297**, 681–683.

Nguyen, P.V., Abel, T. & Kandel, E.R. (1994) Requirement of a critical period of transcription for induction of a late phase of LTP. *Science*, **265**, 1104–1107.

Nguyen, P.V., Duffy, S.N. & Young, J.Z. (2000) Differential maintenance and frequency-dependent tuning of LTP at hippocampal synapses of specific strains of inbred mice. *J. Neurophysiol.*, **84**, 2484–2493.

Nguyen, P.V. & Kandel, E.R. (1997) Brief theta-burst stimulation induces a transcription-dependent late phase of LTP requiring cAMP in area CA1 of the mouse hippocampus. *Learn. Mem.*, **4**, 230–243.

Osaka, H., Wang, Y.-L., Takada, K., Takizawa, S., Setsuie, R., Li, H., Sato, Y., Nishikawa, K., Sun, Y.-J., Sakurai, M., Harada, T., Hara, Y., Kimura, I., Chiba, S., Namikawa, K., Kiyama, H., Noda, M., Aoki, S. & Wada, K. (2003) Ubiquitin carboxy-terminal hydrolase L1 binds to and stabilizes monoubiquitin in neuron. *Human Mol. Genet.*, **12**, 1945–1958.

Saigoh, K., Wang, Y.-L., Suh, J.G., Yamanishi, T., Sakai, Y., Kiyosawa, H., Harada, T., Ichihara, N., Wakana, S., Kikuchi, T. & Wada, K. (1999) Intragenic deletion in the gene encoding ubiquitin carboxy-terminal hydrolase in *gad* mice. *Nat. Genet.*, **23**, 47–51.

Selkoe, D.J. (2002) Alzheimer's disease is a synaptic failure. *Science*, **298**, 789–791.

Shemer, I., Holmgren, C., Min, R., Fulop, L., Zilberter, M., Sousa, K.M., Farkas, T., Hartig, W., Penke, B., Burnashev, N., Tanila, H., Zilberter, Y. & Harkany, T. (2006) Non-fibrillar β-amyloid abates spike-timing-dependent synaptic potentiation at excitatory synapses in layer 2/3 of the neocortex by targeting postsynaptic AMPA receptors. *Eur. J. Neurosci.*, **23**, 2035–2047.

Small, D.H., Mok, S.S. & Bornstein, J.C. (2001) Alzheimer's disease and Aβ toxicity: from top to bottom. *Nat. Rev. Neurosci.*, **2**, 595–598.

Snyder, E.M., Nong, Y., Almeida, C.G., Paul, S., Moran, T., Choi, E.Y., Naim, A.C., Salter, A.W., Lombroso, P.J., Gouras, G.K. & Greengard, P. (2005) Regulation of NMDA receptor trafficking by amyloid-β. *Nat. Neurosci.*, **8**, 1051–1058.

Takamatsu, I., Sekiguchi, M., Wada, K., Sato, T. & Ozaki, M. (2005) Propofol-mediated impairment of CA1 long-term potentiation in mouse hippocampal slices. *Neurosci. Lett.*, **389**, 129–132.

Trinchese, F., Liu, S., Battaglia, F., Walter, S., Mathews, P.M. & Arancio, O. (2004) Progressive age-related development of Alzheimer-like pathology in APP//PS1 mice. *Ann. Neurol.*, **55**, 801–814.

Vitolo, O.V., Sant'Angelo, A., Costanzo, V., Battaglia, F., Arancio, O. & Shelanski, M. (2002) Amyloid β-peptide inhibition of the PKA/CREB pathway and long-term potentiation: reversibility by drugs that enhance cAMP signaling. *Proc. Natl. Acad. Sci. USA*, **99**, 13217–13221.

Wilkinson, K.D., Lee, K.M., Deshpande, S., Duerksen-Hughes, P., Boss, J.M. & Pohl, J. (1989) The neuron-specific protein PGP 9.5 is a ubiquitin carboxyl-terminal hydrolase. *Science*, **246**, 670–673.

Xue, S. & Jia, J. (2006) Genetic association between ubiquitin carboxy-terminal hydrolase-L1 gene S18Y polymorphism and sporadic Alzheimer's disease in a Chinese Han population. *Brain Res.*, **1087**, 28–32.

Yamada, K., Santo-Yamada, Y. & Wada, K. (2003) Stress-induced impairment of inhibitory avoidance learning in female neuromedin B receptor-deficient mice. *Physiol. Behav.*, **78**, 303–309.

Yamada, K., Santo-Yamada, Y., Wada, E. & Wada, K. (2002) Role of bombesin (BN)-like peptides/receptors in emotional behavior by comparison of three strains of BN-like peptide receptor knockout mice. *Mol. Psychiatry*, **7**, 113–117.

Yao, P.J., Zhu, M., Pyun, E.I., Brooks, A.I., Therianos, S., Meyers, V.E. & Coleman, P.D. (2003) Defects in expression of genes related to synaptic vesicle trafficking in frontal cortex of Alzheimer's disease. *Neurobiol. Dis.*, **12**, 97–109.

Yi, J.J. & Ehlers, M.D. (2007) Emerging roles for ubiquitin and protein degradation in neuronal function. *Pharmacol. Rev.*, **59**, 14–39.

Zushida, K., Sakurai, M., Wada, K. & Sekiguchi, M. (2007) Facilitation of extinction learning for contextual fear memory by PEPA-a potentiator of AMPA receptors. *J. Neurosci.*, **27**, 158–166.

Aberrant molecular properties shared by familial Parkinson's disease-associated mutant UCH-L1 and carbonyl-modified UCH-L1

Tomohiro Kabuta[1,2,*], Rieko Setsuie[1,2], Takeshi Mitsui[1,3], Aiko Kinugawa[1], Mikako Sakurai[1], Shunsuke Aoki[1], Kenko Uchida[3] and Keiji Wada[1,*]

[1]Department of Degenerative Neurological Diseases, National Institute of Neuroscience, National Center of Neurology and Psychiatry, 4-1-1 Ogawahigashi, Kodaira, Tokyo 187-8502, Japan, [2]The Japan Health Sciences Foundation, 13-4 Nihonbashi Kodenma, Chuo-ku, Tokyo 103-0001, Japan and [3]Department of Electrical Engineering and Bioscience, Waseda University, Tokyo 169-8555, Japan

Parkinson's disease (PD) is a neurodegenerative disorder characterized by loss of dopaminergic neurons. The I93M mutation in ubiquitin C-terminal hydrolase L1 (UCH-L1) is associated with familial PD, and we have previously shown that the I93M UCH-L1-transgenic mice exhibit dopaminergic cell loss. Over 90% of neurodegenerative diseases, including PD, occur sporadically. However, the molecular mechanisms underlying sporadic PD as well as PD associated with I93M UCH-L1 are largely unknown. UCH-L1 is abundant (1–5% of total soluble protein) in the brain and is a major target of oxidative/carbonyl damage associated with sporadic PD. As well, abnormal microtubule dynamics and tubulin polymerization are associated with several neurodegenerative diseases including frontotemporal dementia and parkinsonism linked to chromosome 17. Here we show that familial PD-associated mutant UCH-L1 and carbonyl-modified UCH-L1 display shared aberrant properties: compared with wild-type UCH-L1, they exhibit increased insolubility and elevated interactions with multiple proteins, which are characteristics of several neurodegenerative diseases-linked mutants. Circular dichroism analyses suggest similar structural changes in both UCH-L1 variants. We further report that one of the proteins interacting with UCH-L1 is tubulin, and that aberrant interaction of mutant or carbonyl-modified UCH-L1 with tubulin modulates tubulin polymerization. These findings may underlie the toxic gain of function by mutant UCH-L1 in familial PD. Our results also suggest that the carbonyl modification of UCH-L1 and subsequent abnormal interactions of carbonyl-modified UCH-L1 with multiple proteins, including tubulin, constitute one of the causes of sporadic PD.

INTRODUCTION

Parkinson's disease (PD) is the most common neurodegenerative movement disorder and is characterized by progressive cell loss confined mostly to dopaminergic neurons in the substantia nigra pars compacta. The I93M mutation in ubiquitin C-terminal hydrolase L1 (UCH-L1) was reported in a German family with dominantly inherited PD (1). To assess the correlation of the I93M mutation and pathogenesis of PD, we have previously generated UCH-L1[I93M]-transgenic mice. These mice exhibited progressive dopaminergic cell loss in the substantia nigra (2), suggesting that the I93M mutation in UCH-L1 is a causative mutation for PD. The S18Y polymorphism in UCH-L1 has been reported to be associated with decreased risk of PD (3). However, it has also been reported that S18Y is not associated with risk of PD (4).

UCH-L1 is abundant (1–5% of total soluble protein) in the brain (5) and is thought to hydrolyse polymeric ubiquitin and ubiquitin conjugates to monoubiquitin (6). UCH-L1 has also been reported to act as a ubiquitin ligase *in vitro* (7). In

*To whom correspondence should be addressed. Tel: +81 423461715; Fax: +81 423461745; Email: kabuta@ncnp.go.jp; clockkab@ybb.ne.jp (T.K.); wada@ncnp.go.jp (K.W.)

addition to these enzymatic activities, we have found that UCH-L1 binds to and stabilizes monoubiquitin in neurons (8). Our previous studies using circular dichroism (CD) and small-angle neutron scattering strongly suggested that the I93M mutation in UCH-L1 alters the conformation of UCH-L1 (9,10). We have previously shown that mice deficient in UCH-L1 do not exhibit progressive dopaminergic cell loss, in contrast to UCH-L1^{I93M}-transgenic mice (2,8,11), suggesting that a loss or decrease in the level of UCH-L1 is not the main cause of PD, and that UCH-L1^{I93M}-associated PD is caused by an acquired toxicity. Thus, although the hydrolase activity of UCH-L1^{I93M} is decreased (1,9), this decreased activity may not be a major cause of PD.

Increased oxidative stress is associated with neurodegenerative diseases (12,13). In sporadic PD brains, UCH-L1 is a major target of carbonyl formation (12), which is the most widely used marker for oxidative damage to proteins. UCH-L1 has also been identified as a component of several inclusion bodies characteristic of neurodegenerative diseases, including Lewy bodies (14). These findings suggest that UCH-L1 and its modification by carbonyl formation are involved in the cause of sporadic PD. Despite the fact that the majority of PD cases occur sporadically, the molecular mechanisms underlying the causes of sporadic PD, as well as UCH-L1^{I93M}-associated PD, are largely unknown. Moreover, the biochemical properties of UCH-L1^{I93M} and carbonyl-modified UCH-L1 in mammalian cells, such as their protein interactions or detergent insolubility (i.e. the amount of a protein in the insoluble fraction), are poorly understood.

In this study, we analyzed the molecular properties of carbonyl-modified UCH-L1 and UCH-L1^{I93M} and elucidated novel properties of UCH-L1 variants, including protein interactions. We show that carbonyl-modified UCH-L1 and UCH-L1^{I93M} share common properties. Our findings provide novel insights into understanding the mechanisms underlying the toxic gain of function by mutant UCH-L1 and suggest that oxidative stress and subsequent protein interactions of carbonyl-modified UCH-L1 constitute one of the causes of sporadic PD. We also discuss the possible involvement of oxidative modifications of UCH-L1 in other neurodegenerative diseases.

RESULTS

Disease-associated mutants including UCH-L1^{I93M} display aberrant insolubility

Aberrantly increased insolubility compared with wild-type protein is a common biochemical feature of several mutant proteins associated with neurodegenerative diseases: for example, mutant α-synuclein associated with familial PD (15), mutant SOD1 associated with familial amyotrophic lateral sclerosis (ALS) (16,17) and mutant tau associated with frontotemporal dementia and parkinsonism linked to chromosome 17 (18). Although we have previously shown that the insolubility of UCH-L1 in the UCH-L1^{I93M}-transgenic mouse brain is increased compared with that in wild-type mouse (2), the insolubility of UCH-L1^{I93M} itself has been unclear. We observed that pathogenic α-synuclein and SOD1 mutant proteins exhibit increased detergent insolubility

in mammalian cells compared with wild-type proteins (Fig. 1A and B). The insolubility of UCH-L1^{I93M} was examined under the same experimental conditions, in which the causative mutants are distinguishable from wild-type proteins. We found that, in dopaminergic SH-SY5Y cells, the protein level of UCH-L1^{I93M} in the insoluble fraction was markedly higher than the levels of UCH-L1^{WT}, UCH-L1^{S18Y}, UCH-L1^{D30K}, which lacks hydrolase activity and binding affinity for ubiquitin (8), and UCH-L1^{C90S}, which lacks hydrolase activity but maintains binding affinity for ubiquitin (8) (Fig. 1C). There was no notable difference among the soluble protein levels (Fig. 1C). The formation of high molecular weight aggregates, which is also a common feature of several mutants, was observed almost exclusively in the insoluble fraction with UCH-L1^{I93M} (Fig. 1C), consistent with the report that UCH-L1^{I93M} produced more aggresomes than UCH-L1^{WT} (19). Increased insolubility of UCH-L1^{I93M} and UCH-L1$^{S18Y/I93M}$ and an increase in the amounts of aggregates specific for these proteins were observed in COS-7 cells (Fig. 1D; Supplementary Material, Fig. S1A), which express very low levels of endogenous UCH-L1. These results demonstrate that UCH-L1^{I93M} shares common features with several mutant proteins linked to neurodegenerative diseases, thus, further supporting the idea that the I93M mutation in UCH-L1 is a causative mutation for PD. Our results also suggest that the insolubility of UCH-L1 is independent of monoubiquitin-binding.

UCH-L1^{I93M} abnormally interacts with multiple proteins

Although increased insolubility is a common characteristic of several mutant proteins associated with neurodegenerative diseases, and this may play a role in the neurotoxicity of the mutant proteins, accumulating evidence suggests that a soluble mutant is the main cause of neurodegeneration (20,21). Studies of dominantly inherited neurodegenerative disease-linked mutants strongly suggest that abnormal physical interactions of the mutant proteins with other proteins constitute a cause of disease (22–26). Hence, we next examined the effect of the I93M mutation on the protein interactions of soluble UCH-L1 using a co-immunoprecipitation (coIP) assay. Silver staining of immunoprecipitant revealed that UCH-L1^{WT} interacts with multiple proteins over 30 kDa (Fig. 1E). We found that the amount of each protein interacting with UCH-L1^{I93M} is mostly higher than the amount interacting with UCH-L1^{WT} or other UCH-L1 variants (Fig. 1F; Supplementary Material, Fig. S1B). Monoubiquitin binding of UCH-L1^{I93M} was decreased compared with that of UCH-L1^{WT} (Fig. 1G), consistent with the decreased hydrolase activity of UCH-L1^{I93M} (1,9). However, the cellular monoubiquitin level in cells expressing UCH-L1^{I93M} was not changed compared with that in cells expressing UCH-L1^{WT} (Fig. 1G). Since UCH-L1^{I93M}-associated PD is presumably caused by an acquired toxicity, the toxic function of UCH-L1^{I93M} may not be mainly mediated by a decreased interaction with monoubiquitin, but rather by aberrantly elevated interactions with multiple other proteins.
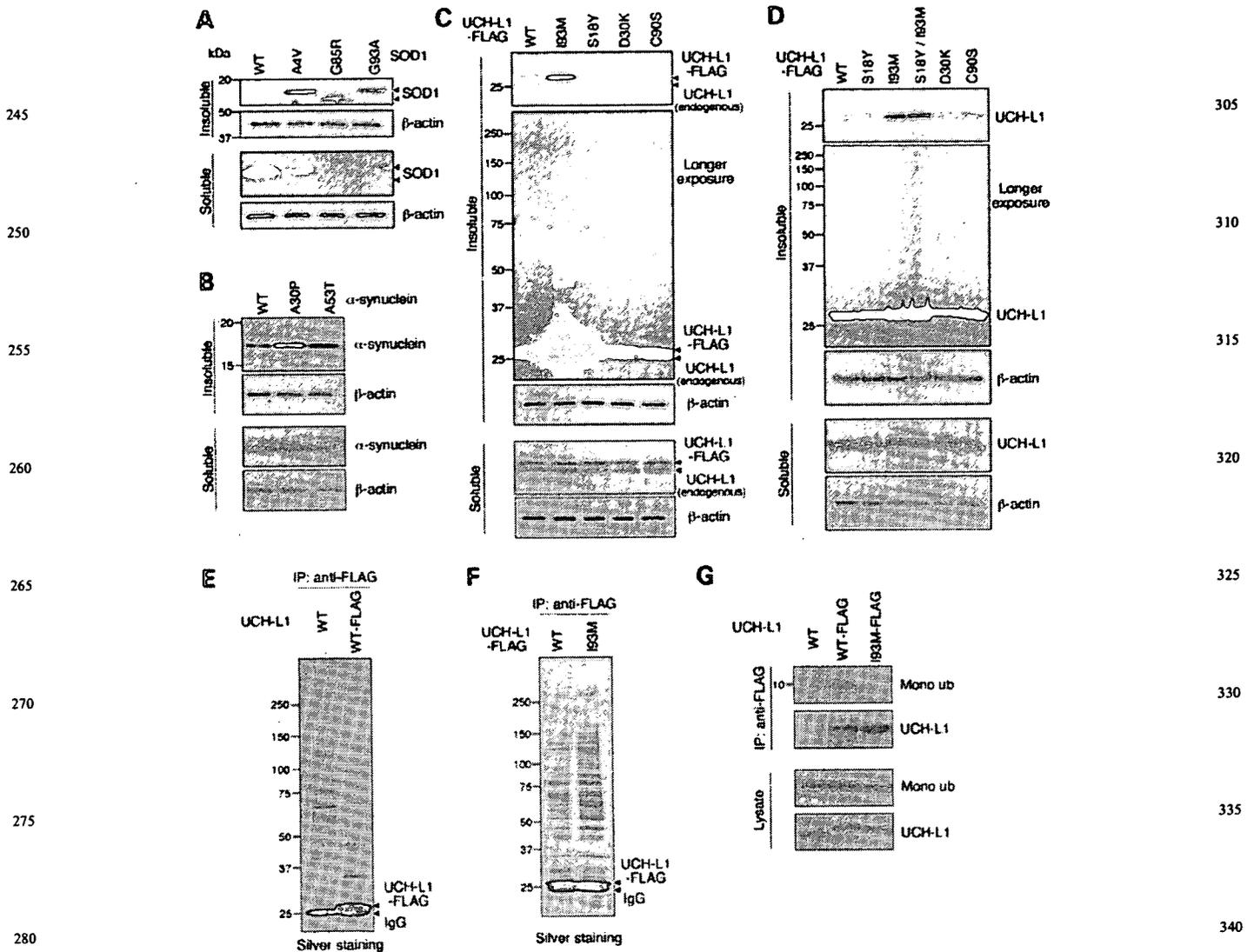
245

250

255

260

265

270

275

280

Figure 1. Aberrant biochemical properties of mutant I93M UCH-L1. [(A)–(D)] SH-SY5Y (A) and (C), Neuro2a (B) and COS-7 cells (D) were transfected with the indicated constructs. Forty-eight hours after transfection, soluble and insoluble fractions were prepared and analyzed by immunoblotting. [(E)–(G)] COS-7 cells were transfected with the indicated constructs. Cell lysates were immunoprecipitated using anti-FLAG antibody and analyzed by silver staining [(E) and (F)] or by immunoblotting (G). In the presence of FLAG-tagged UCH-L1, UCH-L1-interacting proteins were co-immunoprecipitated with UCH-L1 [(E), lane 2], whereas in the absence of FLAG-tagged UCH-L1, proteins were non-specifically precipitated with anti-FLAG beads [(E), lane 1]. Mono ub, monoubiquitin (G).

305

310

315

320

325

330

335

340

345

Carbonyl-modified UCH-L1 exhibits aberrant properties common to UCH-L1[I93M]

In the brains of sporadic PD patients, UCH-L1 is a major target of carbonyl formation (12). Carbonyl groups can be introduced into proteins *in vivo* mainly by reactions with 2-alkenals, 4-hydroxy-2-alkenals (HAE) or ketoaldehydes, which are endogenous aldehydic products formed by lipid peroxidation or glycooxidation (27,28). Protein carbonyls can also be produced by metal-catalyzed reactions with H_2O_2 *in vitro* (28,29). To analyze the biochemical properties of carbonyl-modified UCH-L1, we used several carbonyl compounds or H_2O_2 to modify UCH-L1. We have previously

reported that UCH-L1 is modified by 4-hydroxy-2-nonenal (HNE) *in vitro* (9). In COS-7 cells transfected with UCH-L1[WT], UCH-L1 was modified by physiological concentrations of HNE (10–100 μM) (9) or 4-hydroxy-2-hexenal (HHE) in a dose-dependent manner (Fig. 2A and B; Supplementary Material, Fig. S1C). Carbonyl modification of UCH-L1 was also detected when cells were treated with 100 μM 2-propenal (Fig. 2A), but not with 100 or 500 μM methylglyoxal, 100 or 500 μM malondialdehyde, both of which are ketoaldehydes, or 0.1 or 1 mM H_2O_2 (data not shown). Thus, carbonyl-modified UCH-L1 can be produced by reactions with HAE or 2-alkenals in mammalian cells.

350

355

360

365

425

370

430

375

435

380

440

385

445

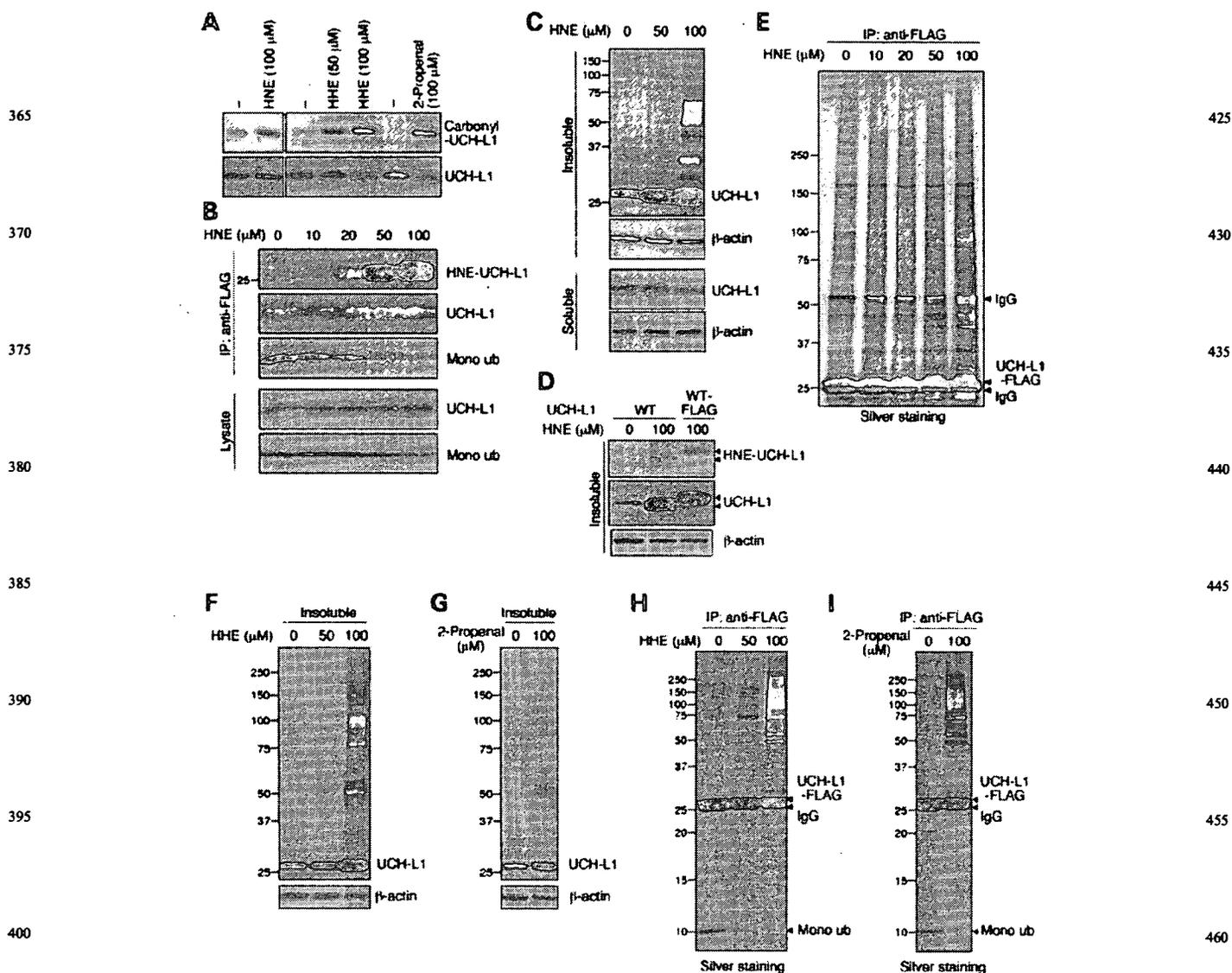390

450

395

455

400

460

Figure 2. Abnormal biochemical properties of carbonyl-modified UCH-L1. (A) COS-7 cells transfected with FLAG-tagged UCH-L1^{WT} were treated with or without the indicated concentrations of carbonyl compounds for 90 min, and immunoprecipitation was performed using anti-FLAG antibody. To detect carbonyl-modified UCH-L1, immunoprecipitants were derivatized with DNPH and immunoblotted using anti-DNP or anti-UCH-L1 antibodies. [(B), (E), (H) and (I)] COS-7 cells transfected with FLAG-tagged UCH-L1^{WT} were treated with the indicated concentrations of HNE [(B) and (E)], HHE (H) or 2-propenal (I) for 90 min, and immunoprecipitation was performed using anti-FLAG antibody. Immunoprecipitants were analyzed by immunoblotting or by silver staining. [(C), (F) and (G)] COS-7 cells transfected with FLAG-tagged UCH-L1^{WT} were treated with the indicated concentrations of HNE (C), HHE (F) or 2-propenal (G). Soluble and insoluble fractions were analyzed by immunoblotting. (D) COS-7 cells transfected with the indicated constructs were treated with or without HNE, and insoluble fractions were prepared. Immunoblotting shows that the insoluble UCH-L1 that is accumulated upon HNE treatment is modified by HNE.

405

465

410

470

Interestingly, carbonyl-modified UCH-L1 and UCH-L1^{I93M} exhibit common biochemical properties: ubiquitin binding of HNE-modified UCH-L1 was decreased (Fig. 2B), and both the insolubility of HNE-modified UCH-L1 and the interactions of HNE-modified UCH-L1 with proteins over 30 kDa were increased, compared with those of UCH-L1^{WT} (Fig. 2C–E). HHE and 2-propenal had similar effects to HNE (Fig. 2F–I). Treatment of cells with 100 μM H$_2$O$_2$, methylglyoxal or malondialdehyde had no effect on the insolubility of UCH-L1 or the interactions of UCH-L1 with other proteins (data not shown). Consistent with the report that UCH-L1 is a major target of carbonyl formation in the brains of sporadic PD patients (12), UCH-L1 is a major target of carbonyl modification in cells treated with HNE (Fig. 3A). We used the EF1 promoter to yield abundant expression of UCH-L1 in this experiment, since the amount of UCH-L1 is 1–5% of
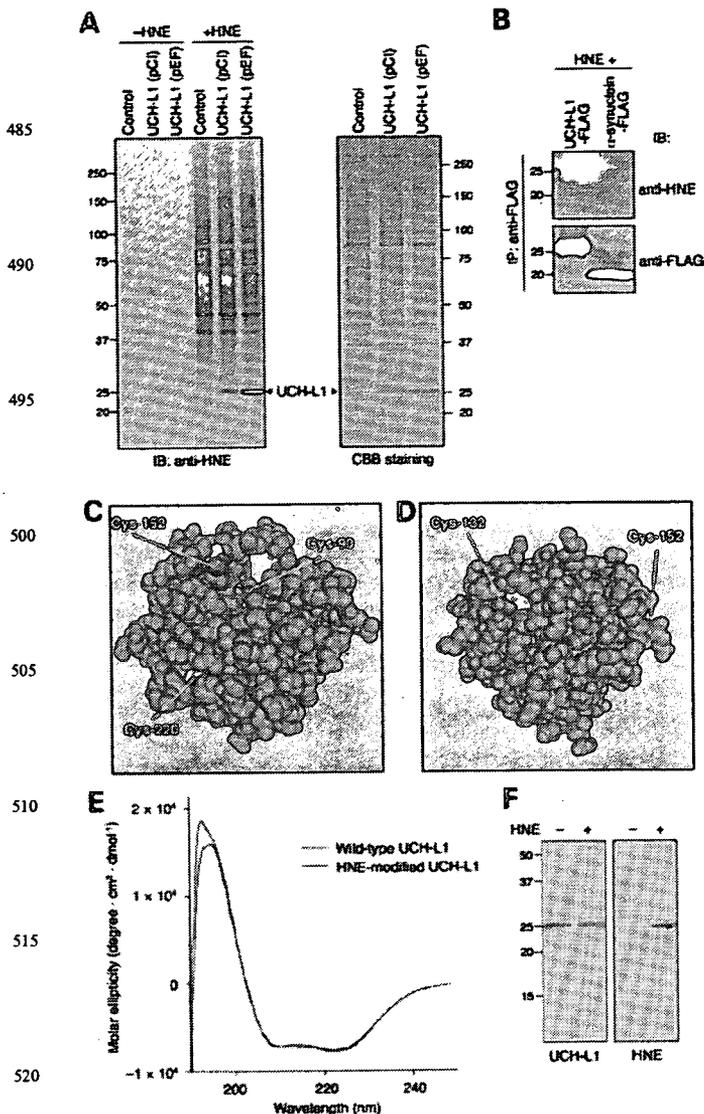
415

420

475

480

Figure 3. Susceptibility of UCH-L1 to HNE modification and structural properties of UCH-L1 variants. (A) COS-7 cells transfected with the indicated constructs were treated with or without 100 μM HNE and analyzed by immunoblotting and CBB staining. (B) COS-7 cells transfected with the indicated constructs were treated with 100 μM of HNE, and immunoprecipitation was performed using anti-FLAG antibody. Immunoprecipitants were analyzed by immunoblotting. [(C) and (D)] Structural model for human UCH-L1. Cys-90, Cys-152 and Cys-220 sidechains are shown in magenta, and backbones are shown in blue (C), using Cn3D software (version 4.1) and NCBI's structural model (mmdbId:38174). Cys-132 and Cys-152 sidechains are shown in magenta, and backbones are shown in blue (D). (E) CD spectra (mean residue ellipticity) for recombinant human UCH-L1 proteins. Wild-type UCH-L1 is shown in red and HNE-modified UCH-L1 in blue. (F) HNE modification of the recombinant UCH-L1 used in (E) was analyzed by immunoblotting. Modification of UCH-L1 by HNE was detected.

soluble protein in the brain (5). These results suggest that the carbonyl-modified UCH-L1 in sporadic PD brains functions as a causative factor for disease in a similar manner to UCH-L1^{I93M}

Cys-90 and Cys-152 of UCH-L1 are targets for HAE modification

The appearance of HNE-modified proteins in nigral neurons has been shown to be associated with sporadic PD (30,31). Therefore, we next determined the HNE-modified amino acid residues of UCH-L1 that regulate its insolubility and protein interactions. HNE can form covalent cross-links with cysteine, lysine and histidine residues in proteins (28). To test the specificity of HNE modification in mammalian cells, we used cells transfected with α-synuclein, which contains no cysteine residues. HNE modification of α-synuclein was not detected when cells were treated with 100 μM HNE (Fig. 3B). These results suggest that among the amino acid residues of UCH-L1, cysteine residues are the primary target for HAE. We speculated that Cys-90 is accessible to HAE, since it is a ubiquitin-binding residue. Using the three-dimensional structure of human UCH-L1 (32), we observed that not only Cys-90 but also Cys-132 and Cys-152 are located on the surface of the protein (Fig. 3C and D). Thus, we tested the insolubility and protein interactions using C90S, C132S and C152S UCH-L1 mutant proteins. We also used C220S UCH-L1 as a control. We found that the C152S mutant bound to monoubiquitin in both HNE-treated cells and untreated cells (Fig. 4A). UCH-L1^{C90S} did not exhibit notably increased insolubility upon HNE-treatment compared with UCH-L1^{WT} (1.3-fold increase in UCH-L1^{C90S}, 2.5-fold increase in UCH-L1^{WT}) (Fig. 4B). The amount of proteins over 30 kDa interacting with UCH-L1^{C90S} was markedly lower than that interacting with UCH-L1^{WT} when cells were treated with HNE (Fig. 4C). Similar results were obtained when cells were treated with HHE (Fig. 4E and F; Supplementary Material, Fig. S1D). Mutations at Cys-132 and Cys-220 had no effect on protein insolubility or interactions (Fig. 4A–C). Consistent with these results, HNE modification of C90S and C152S mutants was decreased compared with that of UCH-L1^{WT} when cells were treated with HNE (~40 and 60% decrease, respectively) (Fig. 4D). These results indicate that HAE modification of UCH-L1 at Cys-90 increases the insolubility and interactions of UCH-L1, and modification of Cys-152 reduces monoubiquitin binding. The level of HNE modification of UCH-L1^{I93M} upon HNE-treatment was markedly lower than that of UCH-L1^{WT} (Fig. 4G). Since the location of Cys-90 is close to Ile-93 (Supplementary Material, Fig. S2), it is possible that the I93M mutation and HAE modification at Cys-90 cause similar structural changes in UCH-L1.

HNE modification causes structural changes in UCH-L1

To address the structural changes in carbonyl-modified UCH-L1, we used CD spectroscopy to estimate the secondary structure. We have previously shown that, compared with UCH-L1^{WT}, the I93M mutant displays lower ellipticity around 195 nm, suggesting a decreased α-helix content, and an increase in the content of β-sheet (9,10). Relative to wild-type protein, HNE-modified UCH-L1 also displayed a lower peak around 190–195 nm (Fig. 3E and F). The relative proportions of α-helix, β-sheet and other secondary structural features in these proteins were estimated from mean residue ellipticity data. HNE-modified UCH-L1 also exhibited
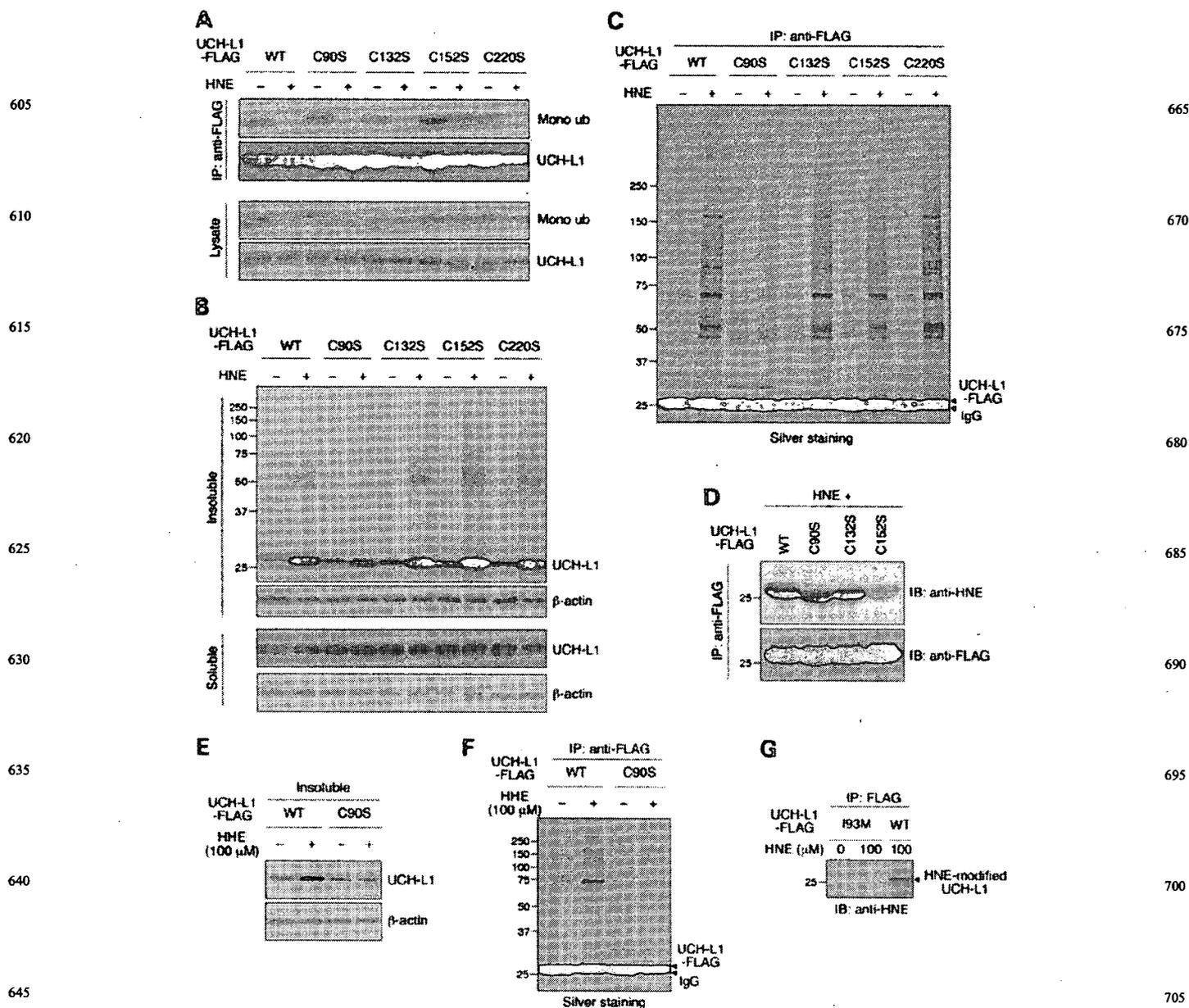
605

610

615

620

625

630

635

640

645

665

670

675

680

685

690

695

700

705

Figure 4. Cysteine residues of UCH-L1 modified by HAE. [(A), (C), (D), (F) and (G)] COS-7 cells transfected with the indicated constructs were treated with or without 100 μM HNE or HHE. Immunoprecipitation was performed using anti-FLAG antibody, and immunoprecipitants were analyzed by immunoblotting or by silver staining. [(B) and (E)] COS-7 cells transfected with the indicated constructs were treated with or without 100 μM HNE or HHE. Soluble and insoluble fractions were analyzed by immunoblotting.

650

decreased α-helix content, and an increase in the content of β-sheet compared with UCH-L1[WT] (42.9% α-helix, 20.9% β-sheet, 20.6% β-turn and 15.7% random for UCH-L1[WT], and 34.0% α-helix, 27.3% β-sheet, 22.3% β-turn and 16.4% random for HNE-modified UCH-L1). These results suggest that UCH-L1[I93M] and carbonyl-modified UCH-L1 adopt a similar aberrant structure.

The ALS-linked mutation in SOD1 increases its hydrophobicity, which may promote aberrant interactions of SOD1 with other cellular constituents (33). However, the inter-

actions of UCH-L1[I93M] or HNE-modified UCH-L1 with hydrophobic beads were not altered relative to those of UCH-L1[WT] (data not shown), indicating that the I93M mutation and HNE modification of UCH-L1 do not increase its hydrophobicity. Considering the fact that unnatural β-sheet proteins readily become insoluble or form further β-hydrogen-bonding with other β-strands they encounter (34), our results suggest that the increased insolubility and protein interactions of abnormal UCH-L1 are due to the increased β-sheet content of UCH-L1.

710

715

720

UCH-L1 physically interacts with tubulin

To understand the molecular mechanism underlying toxic gain of function by UCH-L1, we attempted to identify UCH-L1^{I93M}-interacting proteins by coIP assay and subsequent LC-MS/MS analysis (Fig. 5A). A database search of the peptide sequences obtained identified α-tubulin as a UCH-L1^{I93M}-interacting protein (Supplementary Material, Table S1). The interaction between UCH-L1 and endogenous α-tubulin was confirmed with transiently expressed UCH-L1 (Fig. 5B and C). The interaction of UCH-L1^{I93M} with α-tubulin was increased compared with that of UCH-L1^{WT} (Fig. 5B). We detected the interaction of endogenous α-tubulin with endogenous UCH-L1 using Neuro2a cells (Fig. 5D). Tubulin is composed of a heterodimer of α- and β-tubulin, and we confirmed, using native-PAGE, that tubulin exists as a heterodimer in cell lysates in coIP experimental conditions (data not shown), indicating that UCH-L1 interacts with tubulin. Indeed, β-tubulin was also precipitated with UCH-L1 (Supplementary Material, Fig. S3). In contrast to tubulin, interaction of β-actin with UCH-L1 was not detected (Fig. 5C). To test whether UCH-L1 directly interacts with tubulin, we performed pull-down assay using recombinant UCH-L1 and purified tubulin. Direct interaction of UCH-L1 with tubulin was observed (Fig. 5E).

Since the interactions between UCH-L1 and proteins over 30 kDa are increased by carbonyl modification or I93M mutation of UCH-L1, we tested the effects of HAE on the interaction of UCH-L1 with tubulin. We found that HAE modification of UCH-L1 promotes interactions between UCH-L1 and tubulin (Fig. 5F, G and I). In addition, a coIP assay using C90S, C132S and C152S UCH-L1 mutants showed less binding of UCH-L1^{C90S} to tubulin than UCH-L1^{WT} did, when cells were treated with HNE or HHE (Fig. 5G–I), indicating that the increased interaction of UCH-L1 with tubulin is caused by the HAE modification of Cys-90 of UCH-L1. These results are consistent with the results showing that the HAE modification of Cys-90 of UCH-L1 promotes the interaction of UCH-L1 with multiple proteins. The I93M mutation and HNE modification of UCH-L1 also promote direct interactions between UCH-L1 and tubulin (data not shown). Thus, UCH-L1^{I93M} and HNE-UCH-L1 also exhibit common biochemical properties with respect to the interactions with tubulin.

Both UCH-L1^{I93M} and carbonyl-modified UCH-L1 aberrantly promote tubulin polymerization

Microtubules are dynamic polymers composed of tubulin that continuously grow and shorten through tubulin addition and loss at the microtubule ends. Microtubule-stabilizing agents such as paclitaxel, which promote tubulin polymerization and suppress microtubule dynamics, are effective chemotherapeutic agents for the treatment of many cancers. However, neuropathy is a major adverse effect of microtubule-stabilizing agents-based chemotherapy (35). Paclitaxel induces apoptosis in cortical neurons by a mechanism independent of its cell cycle effects, because postnatal cortical neurons are postmitotic (36). These findings indicate that tubulin polymerization must be tightly regulated for neurons to function and remain

viable. Furthermore, abnormal microtubule dynamics and tubulin polymerization are associated with several neurodegenerative diseases including frontotemporal dementia and parkinsonism linked to chromosome 17 (37,38). Therefore, we examined the effects of UCH-L1^{WT}, UCH-L1^{I93M} and HNE-UCH-L1 on tubulin polymerization using an *in vitro* assay. Interestingly, both UCH-L1^{I93M} and HNE-UCH-L1 promote tubulin polymerization, although UCH-L1^{WT} had almost no effect on it (Fig. 6A and B). Promotion of tubulin polymerization may result in a stabilization of microtubules because of the dynamic instability of microtubules. To test whether abnormal UCH-L1 also promotes tubulin polymerization in mammalian cells, we analyzed the amounts of soluble, polymeric and total tubulin in cells expressing UCH-L1^{I93M}. Although transient expression of UCH-L1^{I93M} had no effect on the amount of total tubulin (Fig. 5B), cells stably expressing UCH-L1^{I93M} contained increased amount of total tubulin compared with control cells or cells expressing other UCH-L1 variants (Fig. 6C). Consistent with the *in vitro* polymerization assay, the amount of polymeric tubulin was increased in cells expressing UCH-L1^{I93M}, whereas the amount of soluble tubulin was not (~1.4 and 1.0-fold increase, respectively, compared with the amount of tubulin in cells expressing UCH-L1^{WT}) (Fig. 6D). The amount of β-actin was not affected by the expression of UCH-L1 variants (Fig. 6C and D), also consistent with the results showing that UCH-L1 does not interact with β-actin. We did not detect specific interaction of UCH-L1 with polymerized tubulin (Fig. 6E), indicating that UCH-L1 may not interact with microtubules, although the possibility is not excluded that they can interact under certain conditions or at a limited number of sites such as the microtubule ends.

Since D30K and C90S mutations had no effect on the interaction of UCH-L1 and tubulin (Fig. 5B), we speculated that the tubulin-binding region of UCH-L1 is different from ubiquitin-binding region. To elucidate the amino acid residues of UCH-L1 involved in the interaction with tubulin and to show that modulation of tubulin polymerization is caused by the increased interaction of UCH-L1 with tubulin, we made a series of alanine substitutions of basic and acidic residues located on the surface of UCH-L1 and performed coIP assays using these mutants (Fig. 7A; Supplementary Material, Fig. S3). The R63A and H185A mutants displayed increased interactions with tubulin (Fig. 7A), indicating that Arg-63 and His-185, which are distinct from the ubiquitin-binding region (Fig. 7B), are involved in this interaction. The increased interactions of R63A and H185A UCH-L1 with tubulin may be caused by altered ionic interactions. In contrast to the I93M mutant or HNE-UCH-L1, the R63A mutant caused a decrease in tubulin polymerization (Fig. 7C). Although UCH-L1^{R63A} has opposite effects to the I93M mutant or HNE-UCH-L1, it also modulated tubulin polymerization. Thus, modulation of tubulin polymerization by UCH-L1 variants is caused by the abnormally increased interaction of UCH-L1 with tubulin.

From our results, we hypothesized that UCH-L1^{I93M}-associated neurodegeneration or PD is at least partly mediated by aberrant tubulin polymerization. Therefore, we tested the effects of UCH-L1^{I93M} and paclitaxel on neuronal cell death using differentiated Neuro2a cells, which
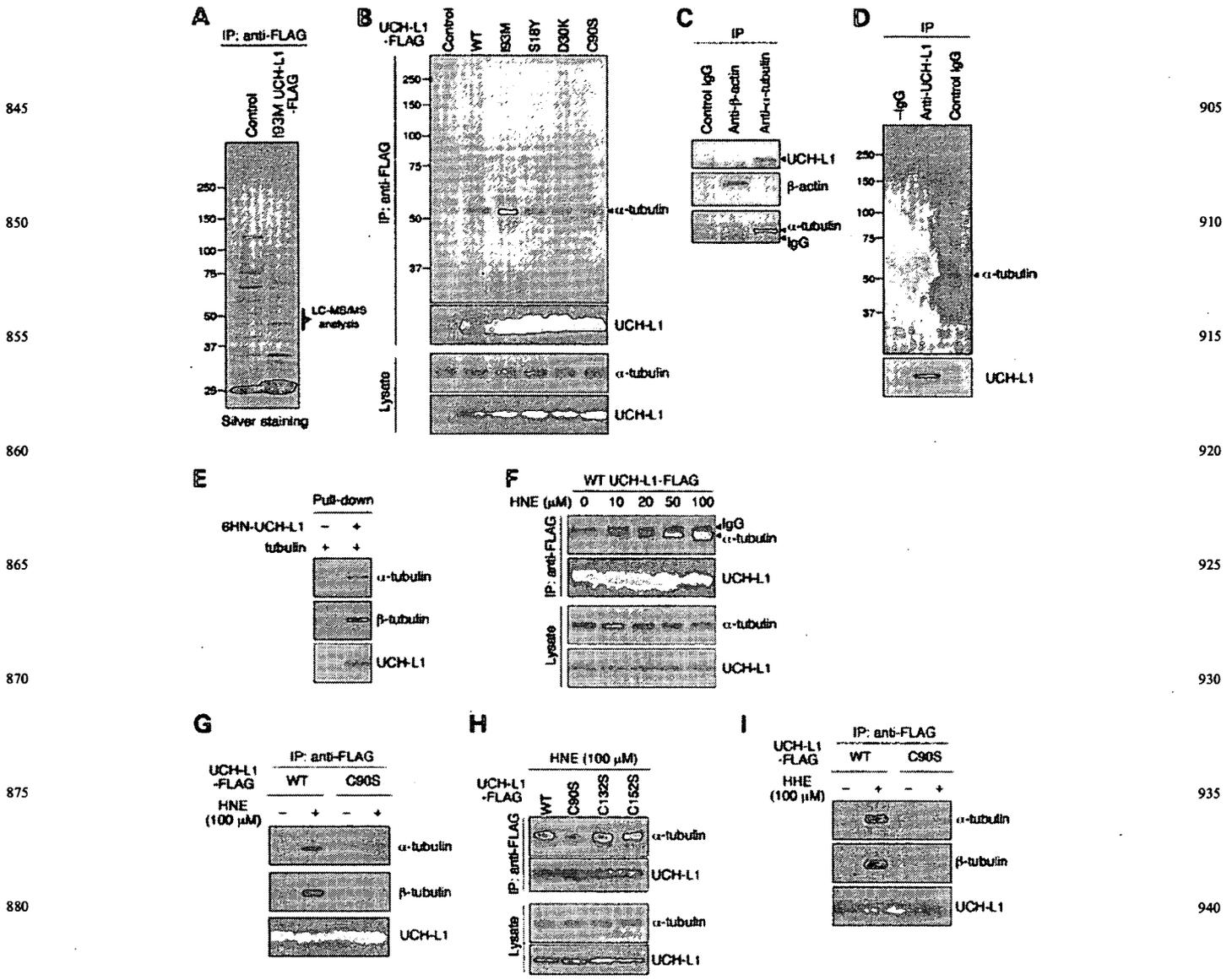
845

905

850

910

855

915

860

920

865

925

870

930

875

935

880

940

Figure 5. Physical interactions of UCH-L1 with tubulin. (**A**) Lysates of HeLa cells transfected with the indicated constructs (control: GFP) were immunoprecipitated with anti-FLAG antibody and analyzed by silver staining. Proteins ~50 kDa in size were subjected to LC-MS/MS analysis. (**B**) Lysates of COS-7 cells transfected with the indicated constructs (control: empty vector) were immunoprecipitated with anti-FLAG antibody and analyzed by immunoblotting. (**C**) Lysates of NIH-3T3 cells stably expressing FLAG-HA-tagged UCH-L1 were immunoprecipitated with the indicated antibodies and analyzed by immunoblotting. (**D**) Lysates of Neuro2a cells were immunoprecipitated with control IgG or anti-UCH-L1 antibody and analyzed by immunoblotting. -IgG, without IgG. (**E**) A pull-down assay was performed using the indicated purified proteins. [(**F**)-(**I**)] COS-7 cells transfected with the indicated constructs were treated with the indicated concentrations of HNE. Lysates were immunoprecipitated with anti-FLAG antibody and analyzed by immunoblotting.

885

945

890

950

have been used to assess the toxicity of mutant proteins linked to neurodegenerative diseases (17,39,40). We confirmed that paclitaxel does not interfere with the interaction between UCH-L1 and tubulin (data not shown). Treatment of cells with 5 μM paclitaxel slightly but significantly elevated cell death in cells expressing UCH-L1[193M], but had no effect in cells expressing UCH-L1[WT] (Fig. 6F). This indicated that the toxicity of UCH-L1[193M] may be at least in part mediated by aberrant microtubule dynamics or tubulin polymerization.

Given that tightly regulated tubulin polymerization is necessary for neurons to be viable, our findings strongly suggest that aberrant tubulin polymerization caused by UCH-L1[193M] underlies the toxic gain of function of mutant UCH-L1, and that carbonyl-modified UCH-L1 also functions as a toxic protein in neurons. We propose that interactions of mutant or carbonyl-modified UCH-L1 with other proteins, including tubulin, constitute one of the causes of not only familial PD, but also sporadic PD (Fig. 7D).
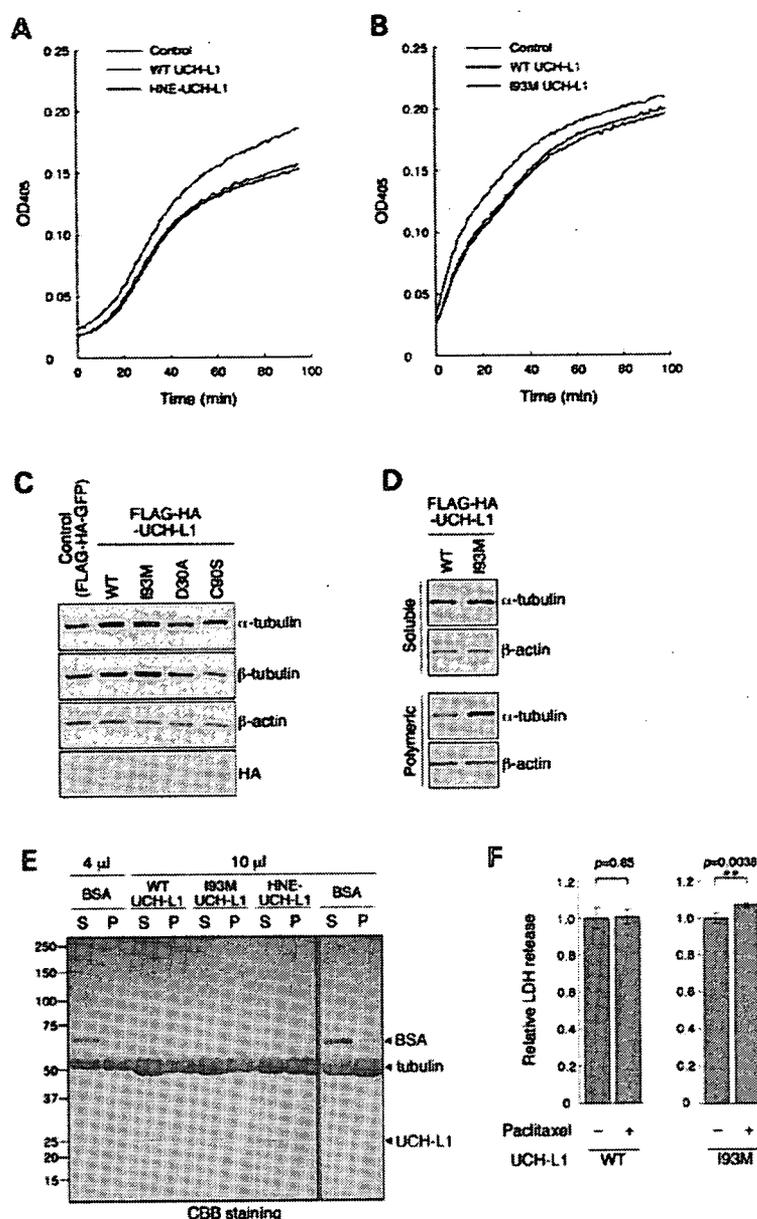
895

955

900

960

965

1025

970

1030

975

1035

980

1040

985

1045

990

1050

995

1055

1000

1060

1005

1065

Figure 6. Effects of the I93M mutation and HNE modification of UCH-L1 on tubulin polymerization. [(A) and (B)] A tubulin polymerization assay was performed in the absence (control) or in the presence of recombinant UCH-L1. The assays were performed at least three times; representative results are shown. [(C) and (D)] Total lysates (C), soluble tubulin fractions and polymeric tubulin fractions (D) of NIH-3T3 cells stably expressing FLAG-HA-tagged UCH-L1 were analyzed by immunoblotting. (E) Interactions of proteins with microtubules. After the tubulin polymerization assay, the polymerized tubulin was pelleted by centrifugation. The indicated volumes of samples from the supernatants (S) and the pellets (P) were analyzed by CBB staining. BSA was used as a control that does not specifically interact with microtubules. The amount of BSA detected in the pellet fraction was approximately one-twelfth of the amount detected in the supernatant fraction. UCH-L1 levels in the pellet fraction were below detectable levels. (F) Differentiated Neuro2a cells transfected with the indicated constructs were incubated with or without 5 μM paclitaxel for 24 h. Cell death was assessed by a lactate dehydrogenase release assay. Data are expressed as the means $\pm$ SD ($n = 4$). **$P < 0.01$ (t-test).

1010

1070

1015

DISCUSSION

Our previous study using CD suggests that the I93M mutation increases the β-sheet content, but reduces the α-helix content of UCH-L1 (9). We have also shown, using small-angle neutron scattering, that UCH-L1^{WT} has an ellipsoidal shape,

whereas UCH-L1^{I93M} has a more globular shape in an aqueous solution (10). However, the biochemical and molecular properties of UCH-L1^{I93M} in mammalian cells, as well as the molecular mechanisms that underlie UCH-L1^{I93M}-associated PD, have not been elucidated. In this study, we have shown that, compared with UCH-L1^{WT}, UCH-L1^{I93M} displays
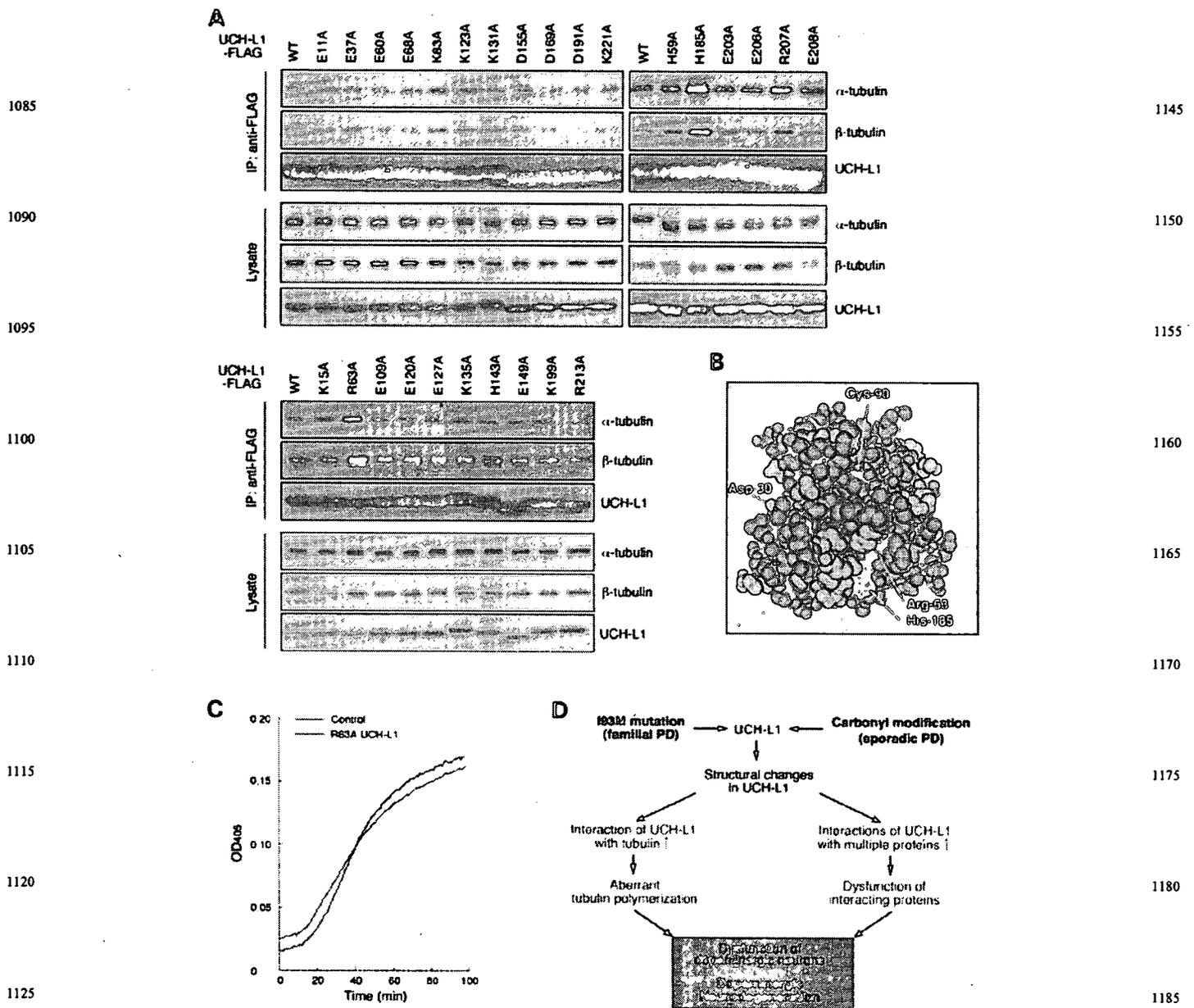
1075

1080

1020

Figure 7. Amino acid residues of UCH-L1 involved in the interaction with tubulin. (A) Alanine-scanning mutagenesis of UCH-L1. Lysates of COS-7 cells transfected with the indicated constructs were immunoprecipitated with anti-FLAG antibody and analyzed by immunoblotting. (B) Structural model for human UCH-L1. Cys-90 is shown in blue, Arg-63 and His-185 are in magenta and basic and acidic amino acid residues that had no effect on tubulin interaction (Figs 5B and7A) are shown in white, using NCBI's structural model (mmdbld:38174). (C) A tubulin polymerization assay was performed in the absence (control) or in the presence of recombinant UCH-L1. (D) Schematic representation of a model for the roles of UCH-L1[193M] and carbonyl-modified UCH-L1 in PD. The 193M mutation (as occurs in familial PD associated with UCH-L1[193M]) and carbonyl modification (as occurs in sporadic PD) cause conformational changes in UCH-L1. Owing to the excess of oxidative stresses including HNE (in the case of sporadic PD) and the abundant expression of UCH-L1 in dopaminergic neurons, abnormal UCH-L1 proteins are overproduced in dopaminergic neurons. Abnormal UCH-L1 interacts with tubulin and aberrantly modulates tubulin polymerization. The aberrant interactions of UCH-L1 variants with multiple proteins may also cause dysfunctions of interacting proteins. The deregulations of abnormal UCH-L1-interacting proteins, including tubulin, result in dysfunction of dopaminergic neurons, leading to neurodegeneration.

increased insolubility, which is characteristic of several neuro-degenerative disease-linked mutants, aberrantly elevated interactions with multiple proteins over 30 kDa and decreased interaction with monoubiquitin (Fig. 1). Taken together, our new and previous findings indicate that the I93M mutation in UCH-L1 alters its conformation, resulting in changes in the biochemical properties of UCH-L1.

Similar to UCH-L1[193M], other dominantly inherited neuro-degenerative disease-linked mutants, such as mutant SOD1 and mutant α-synuclein, cause neurodegeneration, presumably

via an acquired toxicity. Studies of the mutants strongly suggest that abnormally increased interactions of these mutant proteins with other proteins constitute a cause of disease (22–25). Therefore we screened for UCH-L1-interacting proteins using a coIP assay and subsequent LC-MS/MS analysis. We found that tubulin is a novel UCH-L1-interacting protein, and that the interactions of UCH-L1^{I93M} with these proteins are increased compared with those of UCH-L1^{WT} (Fig. 5B). We have also shown that UCH-L1^{I93M} promotes tubulin polymerization and stabilizes microtubules (Fig. 6B–D). UCH-L1^{I93M} and paclitaxel coordinately induced neuronal cell death (Fig. 6F). Together with the fact that tightly regulated tubulin polymerization is essential for neurons to function and remain viable, and that abnormal microtubule dynamics and tubulin polymerization are associated with several neurodegenerative diseases (37,38), our results strongly suggest that aberrant tubulin polymerization caused by mutant UCH-L1 at least partly constitutes a toxic function of mutant UCH-L1. Other than tubulin, mutant UCH-L1 interacts with multiple proteins (Figs 1F and 5A). These other interactors may also be involved in the mechanism of UCH-L1-mediated neurodegeneration (Fig. 7D). We have identified some of these interactors (T.K. and K.W., unpublished data), and these proteins are currently under investigation.

It is known that the majority of PD cases occur sporadically, and that oxidative/carbonyl stresses are elevated in PD brains (12,13). However, the molecular mechanisms underlying the causes of sporadic PD have remained largely unknown. Choi *et al.* (12) have shown that UCH-L1 is a major target of carbonyl damage associated with sporadic PD, implying that carbonyl-modified UCH-L1 is involved in the cause of these sporadic diseases. In the present study, we found that carbonyl-modified UCH-L1 and UCH-L1^{I93M} share molecular and functional properties. Importantly, both UCH-L1s display shared properties in all of the experiments we performed (Supplementary Material, Table S2). These results strongly suggest that carbonyl-modified UCH-L1 is also toxic to neurons and constitutes one of the causes of sporadic PD. Considering that UCH-L1 is abundant in the brain (5), and that UCH-L1 is a major target of carbonyl damage in PD brains (12), it is possible that carbonyl-modified UCH-L1 is the major cause of the disease.

It has been reported that UCH-L1 mRNA is expressed abundantly in dopaminergic neurons in the human brain (41). Abundant expression of UCH-L1 protein in dopaminergic neurons was also observed in mouse brains (Supplementary Material, Fig. S4 and S5). Dopaminergic neurons are particularly exposed to oxidative and carbonyl stresses because dopamine can auto-oxidize into toxic dopamine quinone, superoxide radicals and hydrogen peroxide (42). In addition, it has been reported that oxidative stresses in dopaminergic neurons in sporadic PD brains are higher than the stresses in control brains (30). Thus, in PD, UCH-L1^{I93M} or oxidative/carbonyl-modified UCH-L1 is possibly overproduced in dopaminergic neurons, leading to the selective loss of dopaminergic neurons (Fig. 7D).

Oxidatively modified UCH-L1 has also been found in the brains of both familial and sporadic Alzheimer's disease (AD) patients (12,43,44). AD is characterized pathologically by deposition of the amyloid β-protein in the form of amyloid plaques in the brain, and the deposition of the amyloid β is thought to be a major cause of both familial and sporadic AD (20). Thus, although it is possible that toxicity of carbonyl-modified UCH-L1 is involved in amyloid β-mediated neurodegeneration in AD, carbonyl-modified UCH-L1 may not be the primary cause of AD. A recent report has shown that brains from patients with sporadic PD and AD contain decreased levels of UCH-L1 (30 and 50% decrease, respectively) (12). Gong *et al.* (45) showed that the introduction of exogenous UCH-L1 rescued the synaptic and cognitive functions of AD model mice, which exhibit decreased levels of UCH-L1 in their hippocampi. We have also shown that mice deficient in UCH-L1 exhibit memory dysfunction (46). These findings indicate that a reduction in the levels of functional UCH-L1 may contribute to the pathogenesis of AD. Oxidative modification of several proteins, including antioxidant proteins, is found in mice deficient in UCH-L1 (47), suggesting involvement of these proteins in AD. Since diminution of the proteasome activity may lead to neurodegeneration (48), it is also possible that decreased UCH-L1 function leads to dysfunction of the ubiquitin-proteasome system and this dysfunction contributes to neurodegeneration in AD. On the contrary, mice deficient in UCH-L1 do not exhibit progressive dopaminergic cell loss, indicating that a loss or decrease in the level of UCH-L1 is not the main cause of PD. Investigation of the relationship between the specificity of brain areas that is affected by oxidative stress and genetic or environmental factors should generate further insights into the mechanism of oxidative stress in the pathogenesis of sporadic PD and AD.

In conclusion, familial PD-associated UCH-L1^{I93M} and carbonyl-modified UCH-L1, which is associated with sporadic PD, display common aberrant properties. Thus, UCH-L1^{I93M} is a useful tool for studying the molecular mechanism underlying sporadic PD. We propose that the abnormal interactions of UCH-L1 variants with other proteins including tubulin constitute one of the causes of not only familial PD associated with UCH-L1^{I93M}, but also sporadic PD, and can be therapeutic targets for these diseases and possibly for other neurodegenerative diseases.

MATERIALS AND METHODS

Plasmids

pCI-neo-hUCH-L1 plasmids containing human WT UCH-L1 and UCH-L1 variants with or without FLAG tag were prepared as described previously (49) or generated using a Quik-Change Site-Directed Mutagenesis Kit (Stratagene, La Jolla, CA, USA). The expression plasmid pCR3-hα-synuclein containing FLAG-tagged human α-synuclein was kindly donated by Ryosuke Takahashi (Kyoto University, Kyoto, Japan) and Yuzuru Imai (Tohoku University, Miyagi, Japan) (50). The pcDNA3-hSOD1 expression plasmids containing WT, A4V, G85R or G93A mutant SOD1, and pCI-hα-synuclein expression plasmids containing WT, A30P or A53T mutant α-synuclein were prepared as described previously (17). The expression plasmid pEF-hUCH-L1 containing WT UCH-L1 was constructed by ligating the cDNA

encoding UCH-L1 into pEF-BOS vector (51). The bacterial expression plasmid pPROTetE-hUCH-L1 containing 6HN-tagged UCH-L1 was prepared as described previously. pGEX-hUCH-L1 bacterial expression plasmids containing WT, I93M or R63A UCH-L1 with a GST-tag were constructed by ligating the cDNA encoding each UCH-L1 into pGEX-6P-1 vector (GE Healthcare UK Ltd, Buckinghamshire HP7 9NA, UK).

Cell culture and transfection

Neuro2a, SH-SY5Y, COS-7 and HeLa cells were maintained in Dulbecco's modified Eagle's medium (Sigma, St Louis, MO, USA) supplemented with 10% fetal bovine serum (JRH Biosciences, Lenexa, KS, USA). NIH-3T3 cells stably expressing human UCH-L1 with a FLAG-HA double-tag at the N terminus were cultured as described previously (49). Transient transfection of Neuro2a, SH-SY5Y and COS-7 cells with each vector was performed using the FuGENE 6 Transfection Reagent (Roche Diagnostics, Indianapolis, IN, USA), Trans-Fectin Lipid Reagent (Bio-Rad, Hercules, CA, USA) and Lipofectamine Reagent (Invitrogen, Carlsbad, CA, USA), respectively. For the experiments investigating the carbonyl modification of UCH-L1, cells were incubated at 37°C for 90 min with each carbonyl compound or H_2O_2 in PBS containing 5 mM glucose, 0.3 mM $CaCl_2$ and 0.62 mM $MgCl_2$.

Immunoblotting

SDS–PAGE was performed under reducing conditions. Immunoblotting was performed according to standard procedures. The preparation of detergent (1% Triton X-100)-soluble and -insoluble fractions was performed as described previously (17). Mouse anti-α-tubulin and anti-β-tubulin antibodies were purchased from Sigma. Rabbit anti-α-tubulin and anti-β-tubulin antibodies were from Cell Signaling (Danvers, MA, USA). Mouse anti-HNE and rabbit anti-HNE antibodies were from Oxis (Portland, OR, USA) and Alpha Diagnostic (San Antonio, TX, USA), respectively. Antibodies against SOD1, UCH-L1 and reduced-HNE were purchased from Stressgen Bioreagents (Victoria, BC, Canada), UltraClone (England, UK) and Calbiochem (Darmstadt, Germany), respectively. Anti-β-actin, ubiquitin and FLAG antibodies were from Sigma. The antibody against α-synuclein was from Chemicon (Temecula, CA, USA). For immunoblotting with anti-reduced HNE antibody, the proteins on a PVDF membrane were reduced with 10 mM $NaBH_4$ in Tris-buffered saline for 30 min at room temperature before being reacted with anti-reduced HNE antibody. Carbonyl modification of proteins was detected using an OxyBlot Protein Oxidation Detection Kit (Chemicon) containing an anti-DNP antibody.

Immunoprecipitation

Immunoprecipitation was performed as previously described (52). Cells were harvested by cold immunoprecipitation buffer (15 mM Tris pH 7.5, 120 mM NaCl, 25 mM KCl, 2 mM EGTA, 2 mM EDTA, 0.5% Triton X-100 and protease inhibitors). The lysates were centrifuged at 20 000g for 10 min at 4°C. The supernatant was subjected to immunoprecipitation. Lysates (1 mg protein in immunoprecipitation buffer) were incubated with 5 μg of antibody for 12 h. Twenty microliters of protein G Sepharose (GE Healthcare) was then added, and incubation was continued for 1 h. For the immunoprecipitation of FLAG-tagged proteins, lysates (1–2 mg protein in immunoprecipitation buffer) were incubated with 30 μl anti-FLAG M2 affinity gel (Sigma) for 2 h. After the beads were washed three times with immunoprecipitation buffer, proteins were eluted with SDS sample buffer (10 mM Tris, pH 7.8, 3% SDS, 5% glycerol and 0.02% bromophenol blue). In some experiments, proteins were eluted with SDS sample buffer containing 2% 2-mercaptoethanol. For the immunoprecipitation of endogenous UCH-L1 (Fig. 5D), 100 μg anti-UCH-L1 antibody (53) or 100 μg normal rabbit IgG (Santa Cruz Biotechnology, Santa Cruz, CA, USA) was immobilized to 100 μl of protein G beads using a Seize X Protein G Immnoprecipitation Kit (Pierce, Rockford, IL, USA). Cell lysates (1 mg protein in 50 mM Tris, pH 7.5, 150 mM NaCl, 5 mM EDTA, 0.25% Triton X-100 and protease inhibitors) were incubated with 25 μl of beads for 12 h. Protein G beads without antibody and protein G beads cross-linked with normal rabbit IgG were used as controls.

Mass spectrometry analysis

Protein bands were sliced from the gel and subjected to in-gel trypsin digestion, and LC-MS/MS analysis was performed at APRO Life Science Institute, Inc. (Naruto, Japan) as a custom service.

Circular dichroism

CD measurements of 0.1 mg/ml (4 μM) of recombinant human UCH-L1 without a tag (Boston Biochem, Cambridge, MA, USA) in 20 mM sodium phosphate buffer (pH 8.0) were performed as described previously (9,10). Since two cysteine residues in UCH-L1, Cys-90 and Cys-152, are major targets of HNE modification (Fig. 4), 4 μM UCH-L1 was reacted with 8 μM HNE. Far UV CD spectra (190–250 nm) were recorded in a 1 mm quartz cuvette on a Jasco J-820 spectropolarimeter (Jasco, Tokyo, Japan) equipped with a temperature controller by scanning at a rate of 50 nm/min at 25°C. For all spectra, 12 scans were averaged. All CD spectra were corrected by background subtraction of the spectrum obtained with buffer alone and smoothed. Spectra were analyzed for the percentage of secondary structural elements by a computer program, based on an algorithm that compares experimental spectra with those of known proteins (54).

Preparation of recombinant proteins

6HN-tagged human UCH-L1 proteins were prepared as described previously (9). For purification of UCH-L1 without a tag, the pGEX UCH-L1 vectors were transformed into *Escherichia coli* BL21. Production of fusion proteins was induced by the addition of isopropyl-β-D-thiogalactopyranoside to a final concentration of 0.5 mM. After a 4 h induction at 37°C, the cells were harvested and lysed by sonication in PBS containing 1% Triton X-100 and protease inhibitors. Puri-

fication of GST-tagged UCH-L1 was performed using gluta-thione Sepharose 4B (GE Healthcare), and UCH-L1 was released from GST by digestion using PreScission Protease (GE Healthcare). Purified proteins were resolved by SDS–PAGE under reducing conditions and visualized by Coomassie brilliant blue R-250 to confirm purity (Supplementary Material, Fig. S6).

Pull-down assay

TALON resin (Clontech, Palo Alto, CA, USA) was blocked with 3% BSA for 1 h in order to prevent non-specific binding of tubulin (data not shown) and washed three times with PBS containing 0.05% Triton X-100. Five micrograms of recombinant UCH-L1 with an HN tag and 5 μg of purified tubulin (>99% pure tubulin, Cytoskeleton, Denver, CO, USA) were mixed and incubated for 4 h in PBS containing 0.05% Triton X-100. As a control, vehicle was mixed instead of UCH-L1. Twenty microliters of TALON resin blocked with BSA was then added, and incubation was continued for 1 h. After beads were washed three times with PBS containing 0.05% Triton X-100, proteins were eluted with SDS sample buffer.

Tubulin polymerization assay

An *in vitro* tubulin polymerization assay was performed using a tubulin polymerization assay kit, OD based, >99% pure tubulin (Cytoskeleton), according to the manufacturer's proto-col. Briefly, recombinant UCH-L1 without a tag and tubulin were mixed to give a final concentration of 0.05 mg/ml UCH-L1 and 3 mg/ml tubulin in tubulin polymerization buffer (80 mM PIPES, pH 6.9, 2 mM $MgCl_2$, 0.5 mM EGTA, 1 mM GTP, 5% glycerol) and subjected to a tubulin polymer-ization assay. As a control, vehicle was mixed instead of UCH-L1. Since two cysteine residues in UCH-L1 are major targets of HNE modification (Fig. 4), 40 μM UCH-L1 was reacted with 80 μM HNE to prepare the HNE-modified UCH-L1. To analyze the interaction between UCH-L1 and polymerized tubulin, the polymerized tubulin was pelleted by centrifugation after a tubulin polymerization assay. The supernatant (100 μl) was mixed with 50 μl of 3× SDS sample buffer (30 mM Tris, pH 7.8, 9% SDS, 15% glycerol, 0.06% bromophenol blue). The pellet was washed twice with tubulin polymerization buffer and then dissolved in 150 μl of SDS sample buffer.

Preparation of cell extracts containing soluble and polymeric tubulin

Preparation of soluble and polymeric fractions of tubulin was performed as described (55) with slight modification. Briefly, cells were washed very gently with a microtubule stabilizing buffer (0.1 M N-morpholinoethanesulfonic acid, pH 6.75, 1 mM $MgSO_4$, 2 mM EGTA, 0.1 mM EDTA, 4 M glycerol). Soluble proteins were extracted at 37°C for 5 min in microtu-bule stabilizing buffer containing 0.04% saponin. The remain-ing cytoskeletal fraction in the culture dish was washed with microtubule stabilizing buffer containing 0.4% saponin and dissolved in SDS sample buffer.

Quantitative assessment of cell death

Neuro2a cells were transfected with plasmids. Four hours after transfection, neuronal cell differentiation was induced by addition of 5 mM dibutyryl cAMP as described in the literature (40), and cells were incubated for 24 h. Cells were then incu-bated with or without 5 μM paclitaxel for another 24 h. Cell death was assessed by a lactate dehydrogenase release assay, as described previously (17).

Statistical analysis

For comparison of two groups, the statistical difference was determined by Student's *t*-test.

SUPPLEMENTARY MATERIAL

Supplementary Material is available at HMG Online.

REFERENCES

1. Leroy, E., Boyer, R., Auburger, G., Leube, B., Ulm, G., Mezey, E., Harta, G., Brownstein, M.J., Jonnalagada, S., Chernova, T. *et al.* (1998) The ubiquitin pathway in Parkinson's disease. *Nature*, **395**, 451–452.
2. Setsuie, R., Wang, Y.L., Mochizuki, H., Osaka, H., Hayakawa, H., Ichihara, N., Li, H., Furuta, A., Sano, Y., Sun, Y.J. *et al.* (2007) Dopaminergic neuronal loss in transgenic mice expressing the Parkinson's disease-associated UCH-L1 I93M mutant. *Neurochem. Int.*, **50**, 119–129.
3. Maraganore, D.M., Lesnick, T.G., Elbaz, A., Chartier-Harlin, M.C., Gasser, T., Kruger, R., Hattori, N., Mellick, G.D., Quattrone, A., Satoh, J. *et al.* (2004) UCHL1 is a Parkinson's disease susceptibility gene. *Ann. Neurol.*, **55**, 512–521.
4. Healy, D.G., Abou-Sleiman, P.M., Casas, J.P., Ahmadi, K.R., Lynch, T., Gandhi, S., Muqit, M.M., Foltynie, T., Barker, R., Bhatia, K.P. *et al.* (2006) UCHL-1 is not a Parkinson's disease susceptibility gene. *Ann. Neurol.*, **59**, 627–633.
5. Wilkinson, K.D., Lee, K.M., Deshpande, S., Duerksen-Hughes, P., Boss, J.M. and Pohl, J. (1989) The neuron-specific protein PGP 9.5 is a ubiquitin carboxyl-terminal hydrolase. *Science*, **246**, 670–673.

6. Larsen, C.N., Krantz, B.A. and Wilkinson, K.D. (1998) Substrate specificity of deubiquitinating enzymes: ubiquitin C-terminal hydrolases. *Biochemistry*, 37, 3358–3368.

7. Liu, Y., Fallon, L., Lashuel, H.A., Liu, Z. and Lansbury, P.T., Jr (2002) The UCH-L1 gene encodes two opposing enzymatic activities that affect alpha-synuclein degradation and Parkinson's disease susceptibility. *Cell*, 111, 209–218.

8. Osaka, H., Wang, Y.L., Takada, K., Takizawa, S., Setsuie, R., Li, H., Sato, Y., Nishikawa, K., Sun, Y.J., Sakurai, M. *et al.* (2003) Ubiquitin carboxy-terminal hydrolase L1 binds to and stabilizes monoubiquitin in neuron. *Hum. Mol. Genet.*, 12, 1945–1958.

9. Nishikawa, K., Li, H., Kawamura, R., Osaka, H., Wang, Y.L., Hara, Y., Hirokawa, T., Manago, Y., Amano, T., Noda, M. *et al.* (2003) Alterations of structure and hydrolase activity of parkinsonism-associated human ubiquitin carboxyl-terminal hydrolase L1 variants. *Biochem. Biophys. Res. Commun.*, 304, 176–183.

10. Naito, S., Mochizuki, H., Yasuda, T., Mizuno, Y., Furusaka, M., Ikeda, S., Adachi, T., Shimizu, H.M., Suzuki, J., Fujiwara, S. *et al.* (2006) Characterization of multimetric variants of ubiquitin carboxyl-terminal hydrolase L1 in water by small-angle neutron scattering. *Biochem. Biophys. Res. Commun.*, 339, 717–725.

11. Saigoh, K., Wang, Y.L., Suh, J.G., Yamanishi, T., Sakai, Y., Kiyosawa, H., Harada, T., Ichihara, N., Wakana, S., Kikuchi, T. *et al.* (1999) Intragenic deletion in the gene encoding ubiquitin carboxy-terminal hydrolase in gad mice. *Nat. Genet.*, 23, 47–51.

12. Choi, J., Levey, A.I., Weintraub, S.T., Rees, H.D., Gearing, M., Chin, L.S. and Li, L. (2004) Oxidative modifications and down-regulation of ubiquitin carboxyl-terminal hydrolase L1 associated with idiopathic Parkinson's and Alzheimer's diseases. *J. Biol. Chem.*, 279, 13256–13264.

13. Ischiropoulos, H. and Beckman, J.S. (2003) Oxidative stress and nitration in neurodegeneration: cause, effect, or association? *J. Clin. Invest.*, 111, 163–169.

14. Lowe, J., McDermott, H., Landon, M., Mayer, R.J. and Wilkinson, K.D. (1990) Ubiquitin carboxyl-terminal hydrolase (PGP 9.5) is selectively present in ubiquitinated inclusion bodies characteristic of human neurodegenerative diseases. *J. Pathol.*, 161, 153–160.

15. Lee, M.K., Stirling, W., Xu, Y., Xu, X., Qui, D., Mandir, A.S., Dawson, T.M., Copeland, N.G., Jenkins, N.A. and Price, D.L. (2002) Human alpha-synuclein-harboring familial Parkinson's disease-linked Ala-53 → Thr mutation causes neurodegenerative disease with alpha-synuclein aggregation in transgenic mice. *Proc. Natl Acad. Sci. USA*, 99, 8968–8973.

16. Johnston, J.A., Dalton, M.J., Gurney, M.E. and Kopito, R.R. (2000) Formation of high molecular weight complexes of mutant Cu,Zn-superoxide dismutase in a mouse model for familial amyotrophic lateral sclerosis. *Proc. Natl Acad. Sci. USA*, 97, 12571–12576.

17. Kabuta, T., Suzuki, Y. and Wada, K. (2006) Degradation of amyotrophic lateral sclerosis-linked mutant Cu,Zn-superoxide dismutase proteins by macroautophagy and the proteasome. *J. Biol. Chem.*, 281, 30524–30533.

18. Lewis, J., McGowan, E., Rockwood, J., Melrose, H., Nacharaju, P., Van Slegtenhorst, M., Gwinn-Hardy, K., Paul Murphy, M., Baker, M., Yu, X. *et al.* (2000) Neurofibrillary tangles, amyotrophy and progressive motor disturbance in mice expressing mutant (P301L) tau protein. *Nat. Genet.*, 25, 402–405.

19. Ardley, H.C., Scott, G.B., Rose, S.A., Tan, N.G. and Robinson, P.A. (2004) UCH-L1 aggresome formation in response to proteasome impairment indicates a role in inclusion formation in Parkinson's disease. *J. Neurochem.*, 90, 379–391.

20. Haass, C. and Selkoe, D.J. (2007) Soluble protein oligomers in neurodegeneration: lessons from the Alzheimer's amyloid beta-peptide. *Nat. Rev. Mol. Cell Biol.*, 8, 101–112.

21. Arrasate, M., Mitra, S., Schweitzer, E.S., Segal, M.R. and Finkbeiner, S. (2004) Inclusion body formation reduces levels of mutant huntingtin and the risk of neuronal death. *Nature*, 431, 805–810.

22. Pasinelli, P., Belford, M.E., Lennon, N., Bacskai, B.J., Hyman, B.T., Trotti, D. and Brown, R.H., Jr (2004) Amyotrophic lateral sclerosis-associated SOD1 mutant proteins bind and aggregate with Bcl-2 in spinal cord mitochondria. *Neuron*, 43, 19–30.

23. Zhang, F., Strom, A.L., Fukada, K., Lee, S., Hayward, L.J. and Zhu, H. (2007) Interaction between familial amyotrophic lateral sclerosis (ALS)-linked SOD1 mutants and the dynein complex. *J. Biol. Chem.*, 282, 16691–16699.

24. Urushitani, M., Sik, A., Sakurai, T., Nukina, N., Takahashi, R. and Julien, J.P. (2006) Chromogranin-mediated secretion of mutant superoxide dismutase proteins linked to amyotrophic lateral sclerosis. *Nat. Neurosci.*, 9, 108–118.

25. Cuervo, A.M., Stefanis, L., Fredenburg, R., Lansbury, P.T. and Sulzer, D. (2004) Impaired degradation of mutant alpha-synuclein by chaperone-mediated autophagy. *Science*, 305, 1292–1295.

26. Schaffar, G., Breuer, P., Boteva, R., Behrends, C., Tzvetkov, N., Strippel, N., Sakahira, H., Siegers, K., Hayer-Hartl, M. and Hartl, F.U. (2004) Cellular toxicity of polyglutamine expansion proteins: mechanism of transcription factor deactivation. *Mol. Cell*, 15, 95–105.

27. Uchida, K. (2000) Role of reactive aldehyde in cardiovascular diseases. *Free Radic. Biol. Med.*, 28, 1685–1696.

28. Uchida, K. (2003) Histidine and lysine as targets of oxidative modification. *Amino Acids*, 25, 249–257.

29. Stadtman, E.R. (1993) Oxidation of free amino acids and amino acid residues in proteins by radiolysis and by metal-catalyzed reactions. *Annu. Rev. Biochem.*, 62, 797–821.

30. Yoritaka, A., Hattori, N., Uchida, K., Tanaka, M., Stadtman, E.R. and Mizuno, Y. (1996) Immunohistochemical detection of 4-hydroxynonenal protein adducts in Parkinson disease. *Proc. Natl Acad. Sci. USA*, 93, 2696–2701.

31. Castellani, R.J., Perry, G., Siedlak, S.L., Nunomura, A., Shimohama, S., Zhang, J., Montine, T., Sayre, L.M. and Smith, M.A. (2002) Hydroxynonenal adducts indicate a role for lipid peroxidation in neocortical and brainstem Lewy bodies in humans. *Neurosci. Lett.*, 319, 25–28.

32. Das, C., Hoang, Q.Q., Kreinbring, C.A., Luchansky, S.J., Meray, R.K., Ray, S.S., Lansbury, P.T., Ringe, D. and Petsko, G.A. (2006) Structural basis for conformational plasticity of the Parkinson's disease-associated ubiquitin hydrolase UCH-L1. *Proc. Natl Acad. Sci. USA*, 103, 4675–4680.

33. Tiwari, A., Xu, Z. and Hayward, L.J. (2005) Aberrantly increased hydrophobicity shared by mutants of Cu,Zn-superoxide dismutase in familial amyotrophic lateral sclerosis. *J. Biol. Chem.*, 280, 29771–29779.

34. Richardson, J.S. and Richardson, D.C. (2002) Natural beta-sheet proteins use negative design to avoid edge-to-edge aggregation. *Proc. Natl Acad. Sci. USA*, 99, 2754–2759.

35. Lee, J.J. and Swain, S.M. (2006) Peripheral neuropathy induced by microtubule-stabilizing agents. *J. Clin. Oncol.*, 24, 1633–1642.

36. Figueroa-Masot, X.A., Hetman, M., Higgins, M.J., Kokot, N. and Xia, Z. (2001) Taxol induces apoptosis in cortical neurons by a mechanism independent of Bcl-2 phosphorylation. *J. Neurosci.*, 21, 4657–4667.

37. Panda, D., Samuel, J.C., Massie, M., Feinstein, S.C. and Wilson, L. (2003) Differential regulation of microtubule dynamics by three- and four-repeat tau: implications for the onset of neurodegenerative disease. *Proc. Natl Acad. Sci. USA*, 100, 9548–9553.

38. Fanara, P., Banerjee, J., Hueck, R.V., Harper, M.R., Awada, M., Turner, H., Husted, K.H., Brandt, R. and Hellerstein, M.K. (2007) Stabilization of hyperdynamic microtubules is neuroprotective in amyotrophic lateral sclerosis. *J. Biol. Chem.*, 282, 23465–23472.

39. Tam, S., Geller, R., Spiess, C. and Frydman, J. (2006) The chaperonin TRiC controls polyglutamine aggregation and toxicity through subunit-specific interactions. *Nat. Cell Biol.*, 8, 1155–1162.

40. Kitamura, A., Kubota, H., Pack, C.G., Matsumoto, G., Hirayama, S., Takahashi, Y., Kimura, H., Kinjo, M., Morimoto, R.I. and Nagata, K. (2006) Cytosolic chaperonin prevents polyglutamine toxicity with altering the aggregation state. *Nat. Cell Biol.*, 8, 1163–1170.

41. Solano, S.M., Miller, D.W., Augood, S.J., Young, A.B. and Penney, J.B., Jr (2000) Expression of alpha-synuclein, parkin, and ubiquitin carboxy-terminal hydrolase L1 mRNA in human brain: genes associated with familial Parkinson's disease. *Ann. Neurol.*, 47, 201–210.

42. Lotharius, J. and Brundin, P. (2002) Pathogenesis of Parkinson's disease: dopamine, vesicles and alpha-synuclein. *Nat. Rev. Neurosci.*, 3, 932–942.

43. Castegna, A., Aksenov, M., Aksenova, M., Thongboonkerd, V., Klein, J.B., Pierce, W.M., Booze, R., Markesbery, W.R. and Butterfield, D.A. (2002) Proteomic identification of oxidatively modified proteins in Alzheimer's disease brain. Part I: creatine kinase BB, glutamine synthase, and ubiquitin carboxy-terminal hydrolase L-1. *Free Radic. Biol. Med.*, 33, 562–571.

44. Butterfield, D.A., Gnjec, A., Poon, H.F., Castegna, A., Pierce, W.M., Klein, J.B. and Martins, R.N. (2006) Redox proteomics identification of

oxidatively modified brain proteins in inherited Alzheimer's disease: an initial assessment. *J. Alzheimers Dis.*, **10**, 391–397.

45. Gong, B., Cao, Z., Zheng, P., Vitolo, O.V., Liu, S., Staniszewski, A., Moolman, D., Zhang, H., Shelanski, M. and Arancio, O. (2006) Ubiquitin hydrolase Uch-L1 rescues beta-amyloid-induced decreases in synaptic function and contextual memory. *Cell*, **126**, 775–788.
46. Sakurai, M., Sekiguchi, M., Zushida, K., Yamada, K., Nagamine, S., Kabuta, T. and Wada, K. (2008) Reduction of memory in passive avoidance learning, exploratory behavior and synaptic plasticity in mice with a spontaneous deletion in the ubiquitin C-terminal hydrolase L1 gene. *Eur. J. Neurosci.*, in press.
47. Castegna, A., Thongboonkerd, V., Klein, J., Lynn, B.C., Wang, Y.L., Osaka, H., Wada, K. and Butterfield, D.A. (2004) Proteomic analysis of brain proteins in the gracile axonal dystrophy (gad) mouse, a syndrome that emanates from dysfunctional ubiquitin carboxyl-terminal hydrolase L-1, reveals oxidation of key proteins. *J. Neurochem.*, **88**, 1540–1546.
48. Halliwell, B. (2006) Proteasomal dysfunction: a common feature of neurodegenerative diseases? Implications for the environmental origins of neurodegeneration. *Antioxid. Redox Signal.*, **8**, 2007–2019.
49. Sakurai, M., Ayukawa, K., Setsuie, R., Nishikawa, K., Hara, Y., Ohashi, H., Nishimoto, M., Abe, T., Kudo, Y., Sekiguchi, M. *et al.* (2006)

50. Imai, Y., Soda, M. and Takahashi, R. (2000) Parkin suppresses unfolded protein stress-induced cell death through its E3 ubiquitin-protein ligase activity. *J. Biol. Chem.*, **275**, 35661–35664.
51. Mizushima, S. and Nagata, S. (1990) pEF-BOS, a powerful mammalian expression vector. *Nucleic Acids Res.*, **18**, 5322.
52. Kabuta, T., Hakuno, F., Asano, T. and Takahashi, S. (2002) Insulin receptor substrate-3 functions as transcriptional activator in the nucleus. *J. Biol. Chem.*, **277**, 6846–6851.
53. Sano, Y., Furuta, A., Setsuie, R., Kikuchi, H., Wang, Y.L., Sakurai, M., Kwon, J., Noda, M. and Wada, K. (2006) Photoreceptor cell apoptosis in the retinal degeneration of Uchl3-deficient mice. *Am. J. Pathol.*, **169**, 132–141.
54. Yang, J.T., Wu, C.S. and Martinez, H.M. (1986) Calculation of protein conformation from circular dichroism. *Methods Enzymol.*, **130**, 208–269.
55. Joshi, H.C. and Cleveland, D.W. (1989) Differential utilization of beta-tubulin isotypes in differentiating neurites. *J. Cell Biol.*, **109**, 663–673.

Ubiquitin C-terminal hydrolase L1 regulates the morphology of neural progenitor cells and modulates their differentiation. *J. Cell Sci.*, **119**, 162–171.